UNIVERSITY OF TARTU

Faculty of Science and Technology

Institute of Bioengineering

Sofiya Babok

The role of the viral E1 and E2 proteins in the stable replication of human papillomavirus type 5 genome

Master's Thesis (30 ECTS)

Curriculum Bioengineering

Supervisor:

Assoc. Prof., PhD. Alla Piirsoo

Tartu 2025

The role of the viral E1 and E2 proteins in the stable replication of human papillomavirus type 5 genome

Abstract

Beta human papillomavirus (HPV) infections are associated with cutaneous squamous cell carcinomas in immunocompromised individuals. There is currently no treatment or vaccines targeting beta HPVs. The oncoprogression is dependent on persistent infections, and despite their clinical relevance, the mechanisms of the persistent beta-HPV replication remain poorly understood.

In this study, we aimed to investigate the role of viral replication proteins E1 and E2 in the establishment and long-term maintenance of the episomal HPV5 genome that represents the best-studied beta HPV type. In a transient system, *E1* and *E2* RNA interference led to a time-dependent decrease in viral genome replication. Cell cycle and viability were unaffected by the *E1* and *E2* silencing. These results confirmed that E1 and E2 are essential for establishing viral genome replication.

Further, we created and characterized a stable cell line bearing the HPV5-E1HA-Nluc-E2Flag genome (H5-Nluc+ cells), as well as compared it to a previously described cell line bearing the HPV5 WT genome (H5+ cells). Southern blot analysis confirmed the episomal nature of viral genomes in both cell lines. H5-Nluc+ cells carried approximately 16-fold more viral genome copies than H5+ cells. During investigation of the physical state of the viral genomes, we observed a previously described dominant oligomeric replicon in H5+ cells that replicates in an E1 and E2-independent manner, while no such replicon was present in the H5-Nluc+ cells. These findings suggest that there are two modes of HPV5 replication, one dependent on the E1 and E2 expression and another supported by host cell machinery, with the latter developing after long-term maintenance of the HPV5 genome. However, whether the E1/E2-independent mode of replication occurs during natural HPV infection remains to be elucidated.

Keywords: replication, human papillomavirus (HPV), chronic infection

CERCS: B230 Microbiology, bacteriology, virology, mycology.

Institute name: Institute of Technology

Research group: Molecular virology laboratory

Viiruslike E1 ja E2 valkude roll inimese papilloomiviiruse tüüp 5 genoomi stabiilses replikatsioonis

Lühikokkuvõte

Inimese beeta papilloomiviiruste (HPV) nakkused on seotud naha lamerakk-kartsinoomide tekkega immuunpuudulikkusega isikutel. Hetkel puuduvad beeta-HPV-de vastu suunatud ravimid või vaktsiinid. Onkogeenne progresseerumine sõltub HPV-de pikaajalisest persistentsest nakkusest, kuid vaatamata nende kliinilisele olulisusele on beeta-HPV-de stabiilse replikatsiooni mehhanismid endiselt halvasti mõistetud.

Käesolevas uuringus oli meie eesmärk uurida viiruse replikatsiooni valkude E1 ja E2 rolli episomaalse HPV5 genoomi kujunemisel ja säilitamisel – HPV5 on seni kõige põhjalikumalt uuritud beeta-HPV tüüp. Transientse replikatsiooni mudelis viis E1 ja E2 RNA-vaheline vaigistamine ajas sõltuva viiruse genoomi replikatsiooni vähenemiseni. Rakutsükli kulg ja rakkude eluvõime ei olnud mõjutatud E1 ja E2 vaigistamisest. Need tulemused kinnitasid, et E1 ja E2 on viiruse genoomi replikatsiooni alustamiseks hädavajalikud.

Lisaks lõime ja iseloomustasime stabiilse rakuliini, mis kandis HPV5-E1HA-Nluc-E2Flag genoomi (H5-Nluc+ rakud), ning võrdlesime seda varem kirjeldatud rakuliiniga, mis kandis HPV5 metsiktüüpi genoomi (H5+ rakud). Southern blot analüüs kinnitas viiruse genoomide episomaalset iseloomu mõlemas rakuliinis. H5-Nluc+ rakkudes oli ligikaudu 16 korda rohkem viiruse genoomi koopiaid kui H5+ rakkudes. Viiruse genoomide füüsilise seisundi uurimisel täheldasime H5+ rakkudes eelnevalt kirjeldatud domineerivat oligomeerset replikoni, mis paljuneb E1- ja E2-sõltumatult, samas kui H5-Nluc+ rakkudes sellist replikoni ei esinenud. Need tulemused viitavad, et HPV5-l on kaks replikatsiooni mehhanismi: üks, mis sõltub E1 ja E2 ekspressioonist, ja teine, mida toetab peremeesraku replikatsiooni masinavärk ning mis tekib pärast HPV5 genoomi pikaajalisel säilumisel peremeesrakus. Siiski jääb selgitamata, kas E1/E2-sõltumatu replikatsioonimehhanism toimub loodusliku HPV nakkuse ajal.

Võtmesõnad: replikatsioon, inimese papilloomiviirus (HPV), krooniline infektsioon

CERCS: B230 Mikrobioloogia, bakterioloogia, viroloogia, mükoloogia.

TABLE OF CONTENTS

TERMS, ABBREVIATIONS AND NOTATIONS

AP - alkaline phosphatase

ATP - adenosine triphosphate

cDNA - complementary DNA

CIN - cervical intraepithelial neoplasia

cSCC - cutaneous squamous cell carcinoma

DBD - DNA binding domain

DDR - DNA damage response

DNA - deoxyribonucleic acid

dNTPs - deoxynucleoside triphosphates

DR - dominant replicon

DTT - dithiothreitol

ECM - extracellular matrix

EDTA - ethylenediaminetetraacetic acid

EV - epidermodysplasia verruciformis

FCS - fetal calf serum

Flag-tag - peptide protein tag with DYKDDDDK sequence

GAPDH - glyceraldehyde 3-phosphate dehydrogenase

HA-tag - human influenza hemagglutinin peptide protein tag with YPYDVPDYA sequence

HIV - human immunodeficiency virus

HPV - human papillomavirus

HR - high-risk

HRP - horseradish peroxidase

IC - immunocompromised

IMDM - Iscove's Modified Dulbecco's medium

IP - immunoprecipitation

LCR - long control region

LMW - low molecular weight

LR - low-risk

ND10 - nuclear domain 10 bodies

NES - nuclear export signal

NLS - nuclear localization signal

NMSC - non-melanoma skin cancer

ORF - open reading frame

ori - origin of viral replication

PBS - phosphate-buffered saline

PBS-T - phosphate-buffered saline containing 0.1% Tween

PCR - polymerase chain reaction

PI - propidium iodide

PVDF - polyvinylidene fluoride

PVs - papillomaviruses

qPCR - quantitative polymerase chain reaction

RIPA - radio-immunoprecipitation assay buffer

RLU - relative light units

RNA - ribonucleic acid

RNAi - RNA interference

RT - room temperature or reverse transcriptase

SDS - sodium dodecyl-sulfate

SDS-PAGE - sodium dodecyl-sulfate polyacrylamide gel electrophoresis

siRNA - small interfering RNA

SSC - saline-sodium citrate

STI - sexually transmitted disease

TAE - tris-acetate-EDTA

TEMED - tetramethylethylenediamine

URR - upstream regulatory region

UV - ultra violet

WT - wild-type

INTRODUCTION

Papillomaviruses (PVs) are double-stranded DNA viruses that infect epithelial tissues and can lead to various malignancies in humans. While much of the research on human papillomaviruses (HPVs) has focused on high-risk alpha types such as HPV16 and HPV18, which are responsible for the majority of cervical and anogenital cancers, other variants, such as pro-oncogenic cutaneous HPV types, also may play a crucial role in the development of epithelial malignancies. This is particularly evident in non-melanoma skin cancers (NMSC) affecting immunocompromised individuals, such as organ transplant recipients or patients undergoing certain treatments.

Although preventive measures such as vaccination have been highly successful in reducing productive infections by some alpha HPVs (up to 9 types), there are no antivirals for ongoing infections or vaccines targeting cutaneous HPVs, to which a vast majority of HPVs identified so far belong.

A major obstacle in drug development targeting cutaneous HPVs is a lack of cellular models that mimic chronic infection and enable rapid screening of potential drug candidates, as well as a gap in understanding of the mechanisms involved in the regulation of HPV long-term or stable replication, which is a prerequisite for neoplastic changes.

Human primary keratinocytes, as the native host of HPV, are commonly used in HPV research, but they are challenging and expensive to culture. In contrast, U2OS osteosarcoma cells are one of the few cell lines capable of supporting robust replication of multiple HPV types, including HPV5, that represents one of the most-studied and best-described cutaneous pro-oncogenic HPV types. In most other cell types studied, HPV replication may be triggered only by the simultaneous overexpression of two viral proteins — helicase E1 and transcription factor E2.

In this thesis, we focused on the development and characterization of a U2OS-derived HPV5 stable replication model, which mimics a chronic infection observed in clinical settings. Specifically, we aimed to investigate the role of the E1 and E2 proteins in this model to better understand the mechanisms regulating stable HPV5 replication.

This study was performed within the molecular virology research group at the Institute of Technology, University of Tartu.

1 LITERATURE REVIEW

1.1 Introduction to papillomaviruses

Papillomaviridae family consists of non-enveloped double-stranded DNA viruses with circular genomes that infect epithelial tissues of various vertebrate animal species, including humans, macaques, domestic cows, dogs, cats, rodents, birds, and others (Munday *et al.,* 2017; Rector & Van Ranst, 2013). PVs infect keratinocytes in stratified cutaneous or mucosal epithelia (Doorbar *et al.*, 2015). While most infections are asymptomatic and resolve without medical intervention, certain HPVs are associated with benign proliferative lesions, such as condylomas, warts, papillomas, as well as epithelial cancers (Doorbar *et al.,* 2015; McBride, 2024; Myers *et al.*, 2025).

HPVs are classified into five genera: alpha, beta, gamma, mu, and nu, based on their genome structure, particularly the sequence of the *L1* capsid protein gene, and tissue tropism (**Figure 1**) (de Sanjosé *et al.*, 2018; Mlynarczyk-Bonikowska & Rudnicka, 2024). Mu and nu HPVs cause hands and feet warts, whereas beta and gamma HPVs infect cutaneous epithelia (McBride, 2024). Alphapapillomaviruses target both mucosal and cutaneous epithelia, with various types exhibiting oncogenic potential (McBride, 2024). Notably, certain beta HPVs, along with UV exposure and other co-carcinogens, contribute to the development of cutaneous squamous cell carcinoma (cSCC) (Lambert *et al.*, 2020).

Based on their oncogenic potential, HPVs are divided into high-risk (HR) and low-risk (LR) groups. HR HPVs are implicated in the development of cervical, vaginal, vulvar, penile, anal, and head and neck cancers, whereas LR HPVs primarily cause benign lesions such as anogenital warts (McBride, 2024).

1.2 HPV transmission

HPV is primarily transmitted through skin-to-skin or skin-to-mucosa contact (Petca *et al.*, 2020) and is often regarded as the most common sexually transmitted infection (STI). In the United States, the lifetime probability of acquiring HPV by age 45 is estimated to exceed 80% for men and women with at least one sexual partner of the opposite sex (Chesson *et al.*, 2014). While sexual transmission is the most well-documented route, other modes of transmission have been described as well (Petca *et al.*, 2020). For instance, a meta-analysis on HPV prevalence in foreskin samples of asymptomatic healthy infants and children found

that approximately 17.3% tested positive for some type of HPV, indicating the possibility of non-sexual transmission routes, such as horizontal, self-inoculation, and vertical transmission (B. Lee *et al.*, 2017; Petca *et al.*, 2020). Horizontal transmission can occur through fomites, fingers, mouth, and non-sexual skin contact (B. Lee *et al.*, 2017), with various studies exploring these potential routes, including the role of contaminated gynecological equipment in transmission (Gallay *et al.*, 2016). Self-inoculation has been identified as a potential transmission route, as evidenced by studies showing HPV presence in female virgins and non-abused children with genital warts (Mammas *et al.*, 2019; Sun-Kuie *et al.,* 1990). Additionally, vertical transmission to a newborn child is another possible route, occurring through amniotic fluid, placenta, or contact with genital mucosa during vaginal delivery (Petca *et al.*, 2020).

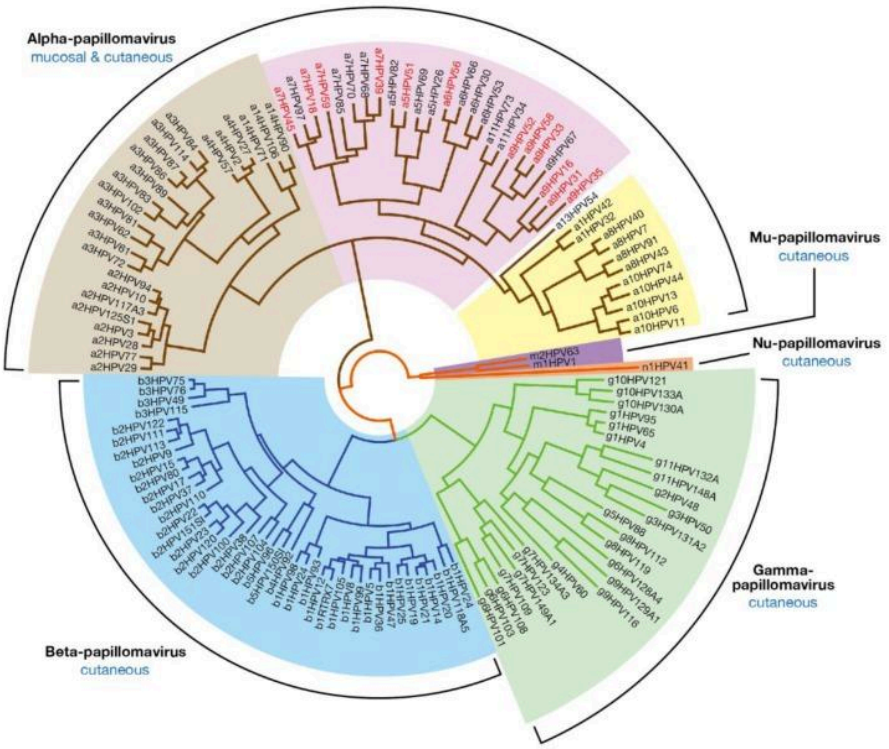

Figure 1. Evolutionary relationships among HPVs, based on alignments of *E1, E2, L1,* and *L2* gene sequences from the PaVE database (Egawa *et al.*, 2015). Alphapapillomaviruses are categorized into LR cutaneous (light brown), LR mucosal (yellow), and HR (pink) based on their oncogenic potential. High-risk types confirmed as human carcinogens are marked in red. The tissue tropisms are indicated as cutaneous or mucosal below the genus name, though exceptions are possible.

Hygiene methods as a prevention strategy for HPV transmission haven't been shown to be effective. HPVs are highly stable, resistant to heat and drying, and can retain 30% infectivity even after seven days of dehydration (Casalegno *et al.*, 2012).

1.3 HPV clinical outcomes

Despite the wide range of transmission modes and viral particle stability, the majority of HPV infections are asymptomatic and often resolve without medical intervention within 6 to 24 months (Petca *et al.*, 2020). Still, various malignancies are associated with papillomavirus infections, ranging from benign warts to anogenital and skin cancers (**Table 1**).

The clinical outcomes of HPV infection vary widely depending on the viral type, site of infection, and certain risk factors. Many infections remain subclinical, with studies reporting a 10-12% overall HPV prevalence in normal cervical cytology samples worldwide (Bruni *et al.*, 2010; de Sanjosé *et al.*, 2007). Other infections may manifest as benign lesions, such as plantar, common, flat, and genital warts, which are predominantly associated with LR HPV types (**Table 1**) (Mlynarczyk-Bonikowska & Rudnicka, 2024). Although these lesions are non-malignant, they can cause significant discomfort, reduce quality of life, and impose a psychological burden (Nahidi *et al.*, 2018; Qi *et al.*, 2014).

A subset of infections, particularly those caused by high-risk HPV types, can persist over time (McBride, 2024). Persistent infection is a critical factor in the development of precancerous lesions and subsequent progression to malignancy (McBride, 2024). It is estimated that HPV infections account for approximately 600,000 cases of cancers annually (Arbyn *et al.*, 2012). They have been associated with nearly 100% of cervical cancers, over 80% of anal cancers, approximately 70% of vaginal cancers, about 40% of vulvar cancers, over 70% of oropharyngeal cancers and about 47% of penile cancers (Arbyn *et al.*, 2012). The 5-year relative survival rate for HPV-associated cancers in the United States has been estimated at around 47-66% (Razzaghi *et al.*, 2018).

One of the most recent findings in HPV malignancies is the involvement of beta HPV types as a cofactor in the development of cutaneous squamous cell carcinoma (cSCC) (Rollison *et al.*, 2019). Beta HPVs contribute to carcinogenesis primarily by interfering with the cellular response to environmental stressors such as ultraviolet (UV) radiation and potentially other carcinogens (Hasche *et al.*, 2017; Rollison *et al.*, 2019; Uberoi *et al.*, 2016). Under physiological conditions, UV exposure induces DNA damage in keratinocytes, leading to

Table 1. The association of different HPV types with selected skin or mucosal lesions (adapted from Mlynarczyk-Bonikowska & Rudnicka, 2024; image sources are listed below the lesion type).

Type of Skin/Mucosal Lesions	HPV Types	Lesion image
plantar warts (image adapted from *Images Library DermNet*)	usually HPV 2, 27, 57, 63, furthermore HPV 1, 4, 10, 41, 65, 88, 95, 60, 65, 66	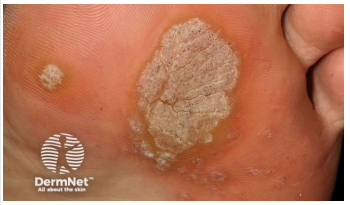
common warts (image adapted from *Images Library DermNet*)	HPV 27, 57, 2, 1, 4	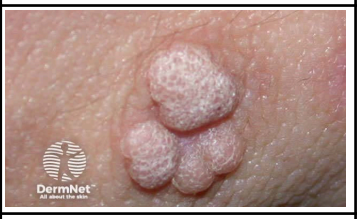
flat warts (image adapted from *Images Library DermNet*)	HPV 3, 10, 26, 27, 28, 29, 77, 78, 94, 114, 41	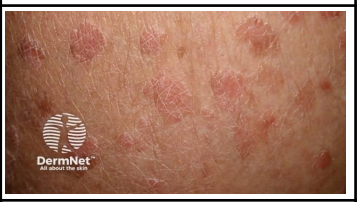
genital warts (Condyloma acuminatum) (image adapted from *Images Library DermNet*)	usually (90%) HPV 6 and 11, less commonly HPV 2, 16, 18, 30–33, 35, 39, 41–45, 51–56, and 59	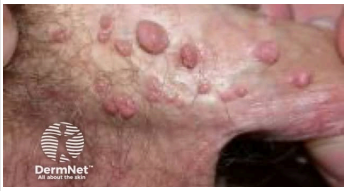
cervical intraepithelial neoplasia (CIN), and cancer (high-grade CIN image is adapted from Palmer & Gillespie, 2010)	HPV 16 (mostly), HPV 18, 31, 33, 35, 39, 45, 51, 52, 56, 58, 59 (carcinogenic), 68 (probably carcinogenic), 26, 53, 66, 67, 69, 70, 73, and 82 (possibly carcinogenic)	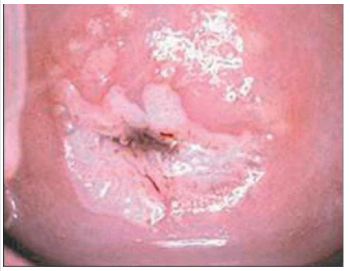
focal epithelial hyperplasia (image adapted from García-Corona *et al.*, 2004)	mainly HPV 13 and 32, but infection or co-infection with other HPVs, such as HPV 6, 11, 16, 18, 31, 39, 40, 51, 52, 55, 58, 66, 68, 69, 71, 74, 90	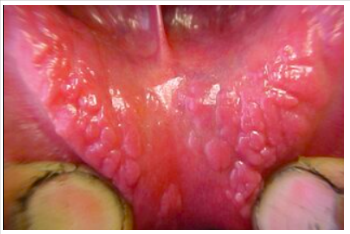
Warts and possible NMSC in EV and IC patients; may be linked to NMSC in the general population (EV image adapted from *Images Library DermNet*)	HPV 5, 8 (possibly carcinogenic), HPV 9, 12, 14, 15, 17, 19–25, 36–38, 47, 49, 75, 76, 80, 92, 93, 96, 98–100, 104, 105, 107, 110, 111, 113, 115, 118, 120, 122, 124, 143, 145	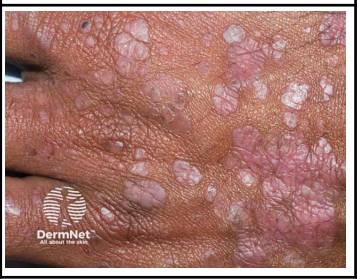

either cell cycle arrest and repair or apoptosis (Lambert *et al.*, 2020). However, expression of E6 and E7 viral proteins from beta HPVs can disrupt these protective mechanisms, promoting the accumulation of DNA mutations and oncoprogression (**Figure 2**) (Lambert *et al.*, 2020).

Another malignancy frequently associated with persistent cutaneous beta HPV infections is Epidermodysplasia Verruciformis (EV) (**Table 1**), a rare skin disorder characterized by the development of wart-like lesions that can progress to cSCC in sun-exposed areas (Rollison *et al.*, 2019). EV can be inherited in an autosomal recessive manner or acquired in immunocompromised individuals, such as patients with HIV or those undergoing immunosuppressive therapy (Myers *et al.*, 2025). Inherited EV is usually caused by mutations in TMC6/EVER1 or TMC8/EVER2 genes, which result in reduced immune response to certain beta HPV infections within keratinocytes (Ramoz *et al.*, 2002). The defective immune response allows persistent viral replication and contributes to malignant transformation in the presence of cofactors such as UV (Patel *et al.*, 2010).

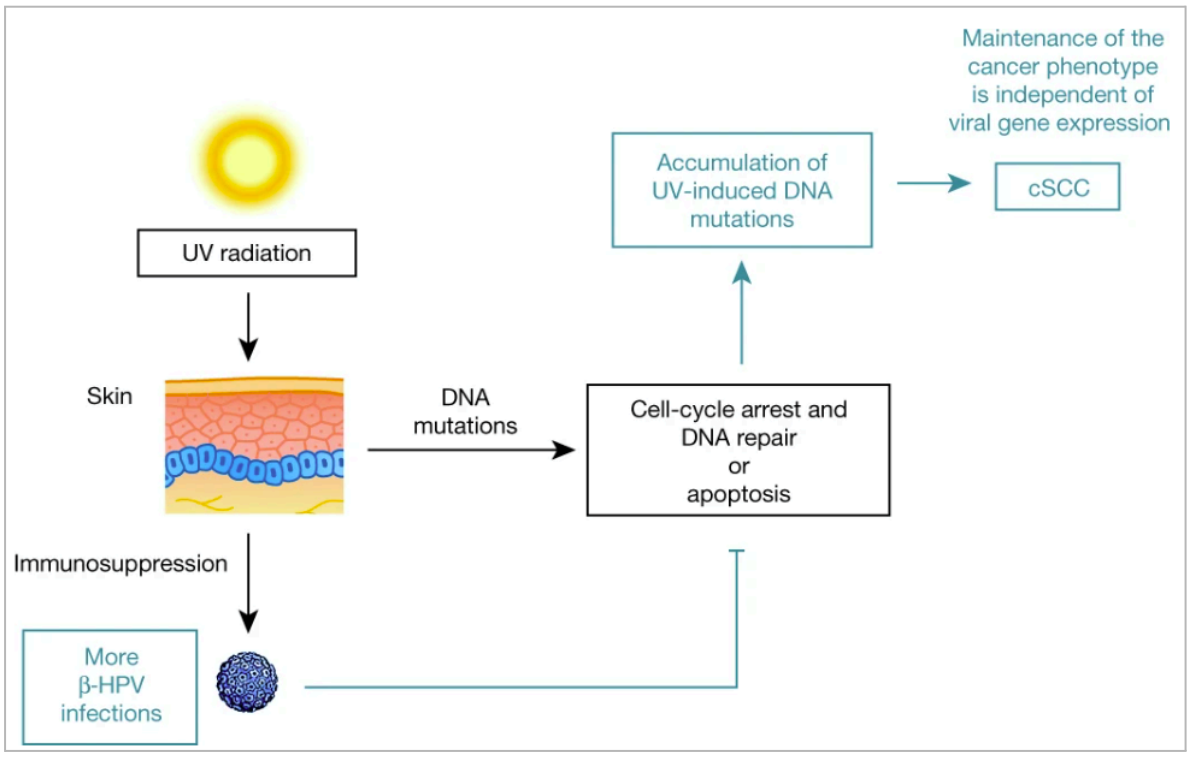

Figure 2. Model for cooperation between some types of beta HPV and UV radiation in promoting cSCCs (Lambert *et al.*, 2020).

While conditions like EV highlight the role of genetic predisposition and immunosuppression in severe HPV outcomes, a range of other risk factors have also been associated with increased risk of HPV infections and disease severity. Behavioural factors include smoking, alcohol consumption, early onset of sexual activity, chronic stress, a high number of sexual partners, and unsafe sex practices (Chelimo *et al.*, 2013; Del Pino *et al.*, 2024; Gheit, 2019; Kuebler *et al.*, 2021; M. Lee *et al.*, 2024). Biological factors such as co-infection with other pathogens and chronic inflammation can further elevate risk (Del Pino *et al.*, 2024; Ebrahimi *et al.*, 2024). Additionally, demographic variables, such as age, sexual orientation, and education level, have been shown to influence the likelihood of HPV infections (Del Pino *et al.*, 2024).

Given the range of factors that influence HPV susceptibility and disease progression, effective treatment strategies are essential, but options remain limited. While multiple vaccines exist to protect against the infections with up to 9 of the most common and harmful mucosal HPV types, there is no treatment available for ongoing HPV infections, and no vaccines targeting cutaneous HPVs (Cheng *et al.*, 2020; de Oliveira *et al.*, 2019).

1.4 HPV infectious life cycle

The HPV life cycle is dependent on keratinocyte differentiation and can be divided into the following stages: viral entry, establishment of viral replication, maintenance replication during the cell cycle, vegetative or productive replication along with host cell differentiation, viral particle assembly, and release of the virus (**Figure 3**) (Gheit, 2019).

To initiate infection, the HPV virion must access the dividing basal cell layer of stratified epithelium, typically through microabrasions or entry via hair follicles, to infect basal keratinocytes or stem epithelial cells (Gheit, 2019; McBride, 2022). The virus initially binds to the heparan sulfate proteoglycans on the cell membrane or on the extracellular matrix (ECM) via major capsid protein L1 (Day & Schelhaas, 2014; Gheit, 2019; McBride, 2022). Laminin-332 has also been shown to act as a transient binding receptor on the ECM, although it appears to be non-essential for viral entry (Day & Schelhaas, 2014). This binding triggers conformational changes in the viral capsid structure and proteolytic cleavage of L1, exposing the amino terminus of the minor capsid protein L2 (Day & Schelhaas, 2014; Feng *et al.*, 2024; Gheit, 2019). Next, the N-terminus of L2 is cleaved, which allows for the HPV capsid to bind to the secondary, currently unidentified, entry receptor (Feng *et al.*, 2024). The virus

is then internalised via endocytosis, and the L2-viral DNA complex, along with a portion of L1, is trafficked to the trans-Golgi network (Day & Schelhaas, 2014; Feng *et al.*, 2024; Gheit, 2019). Within endosomes, the virus undergoes further uncoating, leading to the dissociation of L1 protein from L2 (Day & Schelhaas, 2014; Feng *et al.*, 2024). The L2-viral DNA complex is subsequently transported into the nucleus, which is potentially facilitated by nuclear localisation signals on L2 and involves progression of the host cell through early mitosis (Day & Schelhaas, 2014).

Upon entry into the nucleoplasm, the L2-viral DNA complex localises to nuclear domain 10 (ND10) bodies, which serve as sites of early transcription and replication for many DNA viruses (Gheit, 2019; McBride, 2022). A central region of the L2 protein facilitates tethering of the viral genome to host mitotic chromosomes (Aydin *et al.*, 2017). The HPV replication cycle begins with establishment replication, a phase in which the episomal viral genomes are maintained at approximately 50-400 copies per cell (Doorbar *et al.*, 2015; Gheit, 2019; Hoffmann *et al.*, 2006). Transcripts encoding the viral E1 and E2 proteins are initiated by cellular factors, and once E1 and E2 proteins are synthesized, E2 recruits E1 to the viral origin of replication (ori), where E1 unwinds it, allowing cellular factors to amplify the viral DNA (Bergvall *et al.*, 2013; Della Fera *et al.*, 2021; Doorbar *et al.*, 2012; McBride, 2017). To evade the host cell immune system and keep the viral genome copy number low, the viral genome amplification is most likely limited by the E8^E2 viral repressor protein that acts as an E2 antagonist in the regulation of viral transcription and replication (Dreer *et al.*, 2017; Gheit, 2019).

Following the establishment of viral replication, the infection progresses to the maintenance replication phase, where a constant number of viral episomal genomes is maintained in the nuclei of undifferentiated, proliferating basal cells (Doorbar *et al.*, 2012). These viral genomes are generally believed to replicate once per S phase in coordination with the host cellular DNA and are tethered to host chromatin via the E2 protein to ensure proper partitioning into the daughter cells during mitosis. However, alternative models of replication have been proposed, suggesting a random-choice replication pattern, in which some viral genomes replicate multiple times per S phase, others only once, and some do not at all (Hoffmann *et al.*, 2006). In parallel, the low-level expression of the viral E6 and E7 oncoproteins occurs during early infection, likely to avoid triggering oncogenic transformation while subtly modulating the host environment (Graham, 2017a). To sustain

the maintenance replication, HPVs have evolved multiple strategies involving interactions of early viral E5, E6, and E7 proteins with various cellular factors and enzymes (Della Fera *et al.*, 2021). These interactions contribute to immune evasion, inhibition of cellular differentiation and apoptosis, prevention of replicative senescence and growth arrest, and promotion of continued cell proliferation (Della Fera *et al.*, 2021). This phase can persist for extended periods, enabling the virus to maintain a reservoir within the basal layer of the epithelium (Doorbar *et al.*, 2012).

As infected basal keratinocytes differentiate and migrate toward the epithelial surface, the HPV genome transitions to productive replication, which is characterized by robust genome amplification, late viral genes expression, and assembly of progeny virions (Doorbar *et al.*, 2012). Since differentiated cells typically lack the replication machinery required for DNA synthesis, HPV hijacks the host DNA damage response (DDR) pathway, primarily through the activity of E6 and E7 oncoproteins (Della Fera *et al.*, 2021). Activation of DDR allows the virus to create specialized nuclear sites, which recruit host repair machinery and facilitate viral replication outside of S phase, avoiding competition with host genomic replication (Bergvall *et al.*, 2013; Della Fera *et al.*, 2021).

Productive replication phase also involves activation of a differentiation-dependent viral promoter, resulting in expression of E4 and E5 viral proteins, as well as higher levels of E1 and E2 (Doorbar *et al.*, 2012; Graham, 2017a, 2017b). Completion of the viral life cycle includes expression of major and minor capsid proteins, L1 and L2. Once viral capsids are assembled around the replicated genomes, virions are released through shedding of the outer epithelia (McBride, 2022).

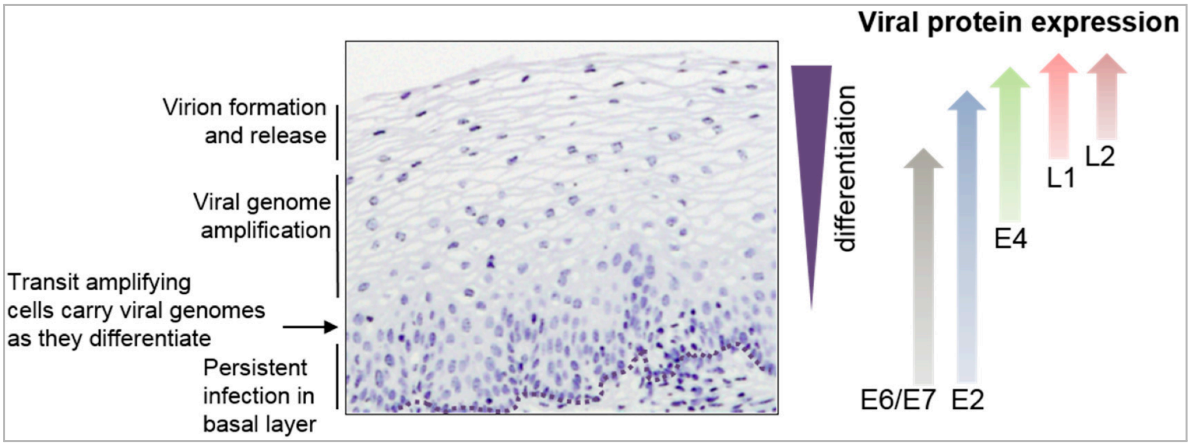

Figure 3. Eosin-stained HPV16-infected cervical epithelium. Nuclei are stained purple.

The key events in viral replication are noted on the left, and viral protein expression patterns are noted on the right (Graham, 2017).

1.5 HPV genome organisation and viral protein functions

The HPV genome is typically 7-8 kb in size and can be divided into three major regions: a non-coding long control region (LCR) or upstream regulatory region (URR), the early region, and the late region (**Figure 4**) (Gheit, 2019). The URR is located upstream of the early region and contains ori, early promoter, and multiple regulatory elements required for viral replication and transcription (Della Fera *et al.*, 2021; Gheit, 2019). The early region can encode the E1, E2, E4, E5, E6, and E7 proteins, which serve various functions in viral gene expression, genome replication, and host cell survival (Gheit, 2019). The late region encodes structural capsid proteins L1 and L2. Only four open reading frames (*E1*, *E2*, *L1*, and *L2*) are considered necessary for replication and shedding of the virus, and are present in all known HPVs (Doorslaer & McBride, 2016). While the general organization is shared among the papillomaviruses, the genome structure and specific functions of encoded proteins may differ between HPV genera or between HR and LR types of HPVs (**Figure 4**). The main functions of individual HPV proteins in viral infections are summarized in **Table 2**.

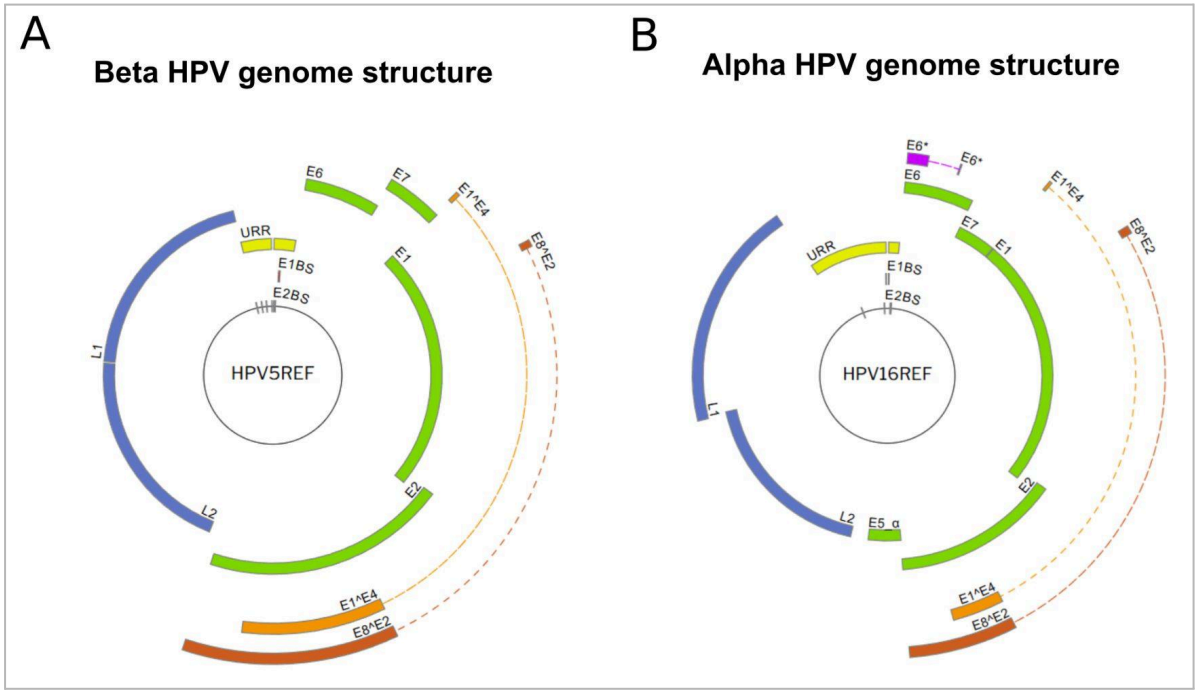

Figure 4. Genome organisation of beta and alpha HPVs. a) HPV5 represents beta HPVs; b) HPV16 represents alpha HPV (images were adapted from *PaVE*). URR is marked in yellow, the early region is highlighted in green, late — in blue.

Table 2. The main functions of HPV proteins during infection. The functions listed are primarily based on studies focusing on high-risk alpha HPVs and may not all be applicable to other genera.

Protein	Main functions during HPV infection
E1	ATP-dependent DNA helicase, essential for viral replication, interacts with cellular DNA replication machinery and other proteins that assist and/or regulate viral replication (Bergvall *et al.*, 2013)
E2	Transcriptional regulator, loads E1 onto ori during replication initiation, tethers viral genomes to host chromosomes in mitosis, enhances viral genomes packaging, can inhibit cell growth and induce apoptosis (McBride, 2013)
E5	Reduces immune detection, promotes cell division, and productive viral replication (McBride, 2022)
E6	Assist in transformation and immortalization of keratinocytes, can inhibit keratinocyte differentiation and interferon response, interacts with various cellular proteins, assists in genome amplification upon differentiation (Vande Pol & Klingelhutz, 2013)
E7	Assist in transformation and immortalization of keratinocytes, support viral replication, disrupt host cell cycle, assist in immune evasion, inhibit apoptosis (Roman & Munger, 2013)
E8^E2	Repress viral transcription and replication (Dreer *et al.*, 2017)
E1^E4	Promote viral genome amplification and viral particle release (McBride, 2022)
L1	Major capsid protein of the HPV virion, interacts with cellular receptors for viral entry (Buck *et al.*, 2013)
L2	Minor capsid protein, facilitates viral encapsidation, host cell entry, vesicular trafficking and escape during infection (Wang & Roden, 2013)

1.6 HPV E1 protein

E1 protein is an ATP-dependent helicase and the only protein with enzymatic activity encoded by HPVs (Bergvall *et al.*, 2013). Its size ranges from approximately 600 to 650 amino acids, depending on the PV type (Bergvall *et al.*, 2013). E1 initiates viral replication by assembling as a double-hexamer at the ori, where it unwinds the DNA and recruits host replication machinery (Morin *et al.*, 2011). It interacts with several cellular proteins involved

in DNA synthesis, including α-DNA polymerase, replication A proteins, topoisomerases I and II, nuclear proliferation cell antigen, and the replication factor C (Bergvall *et al.*, 2013).

Additionally, E1 has been shown to interact with host factors involved in epigenetic processes, which may support viral replication (D. Lee *et al.*, 1999; Swindle & Engler, 1998). Multiple studies have shown that E1 proteins shuttle between the nucleus and cytoplasm to regulate viral replication, utilizing nuclear localisation and nuclear export signals (NLS, NES) (Bergvall *et al.*, 2013). However, during the S phase of the cell cycle, E1 is primarily localized in the nucleus (Bergvall *et al.*, 2013).

Structurally, E1 contains three main functional segments: N-terminal regulatory region, DNA binding domain (DBD), and C-terminal or helicase domain (Bergvall *et al.*, 2013). The N-terminal region is the least conserved and spans roughly 200 amino acids (Bergvall *et al.*, 2013). It contains NLS and NES and has been shown to be essential for optimal replication *in vivo* (Morin *et al.*, 2011). The DBD spans approximately 150 amino acids and binds specific sequences within the viral origin of replication (Bergvall *et al.*, 2013; Castro-Muñoz *et al.*, 2019). Additionally, the DBD contributes to replication through interactions with host factors (Bergvall *et al.*, 2013). The C-terminal enzymatic domain contains a minimal oligomerization domain, an ATPase segment, and a C-terminal brace (Bergvall *et al.*, 2013). It is responsible for E1 oligomerization and DNA unwinding (Bergvall *et al.*, 2013; Côté-Martin *et al.*, 2008). This domain contains conserved motifs required for ATP binding and hydrolysis, and assembles E1 monomers into a functional hexamer (Bergvall *et al.*, 2013; Castella *et al.*, 2006). A flexible C-terminal brace helps to stabilize the oligomer during replication (Bergvall *et al.*, 2013).

The E1 protein plays a crucial role in different stages of the HPV replication cycle (McBride, 2022). It is essential during the initial amplification phase, however, its role in maintenance replication has been found to be more variable (Piirsoo *et al.*, 2020). Studies on mucosal alpha HPV18 and HPV16 have shown that E1 is dispensable for viral replication in stable cell lines, suggesting that host cell machinery may compensate for its function (Egawa *et al.*, 2012; Murakami *et al.*, 2019; Piirsoo *et al.*, 2020). This indicates that mucosal alpha HPV replication involves both E1-dependent and E1-independent mechanisms. Currently, no data is available for stable replication of cutaneous HPV types.

1.7 HPV E2 protein

E2 is a regulatory viral protein, spanning approximately 400 amino acids, that acts as the main viral transcriptional regulator, assists E1 in the initiation of replication, and ensures proper partitioning of viral genomes during cell division (Kurg, 2011; McBride, 2013). E2 regulates viral transcription by binding to specific sequence motifs in the viral genome and recruiting cellular factors that influence transcriptional outcome (McBride, 2013). E2 may act either as a transcriptional activator or repressor depending on a combination of factors, including its expression levels, the context of its binding sites within viral genome and the nature of the recruited cellular factors (Fujii *et al.*, 2001; Graham, 2016; McBride, 2013; Steger & Corbach, 1997).

Additionally, E2 participates in the initiation of viral replication by recruiting the E1 helicase to the ori. This process occurs in two steps: first, E2 cooperatively binds with E1 to form a sequence-specific ori recognition complex. Then, E2 is displaced, and additional E1 molecules are incorporated to form an active double-hexameric helicase (Mohr *et al.*, 1990; Sanders & Stenlund, 1998, 2000).

Beyond its roles in transcription and replication, E2 is also crucial for viral genome maintenance, as it tethers the viral episome to host chromosomes and ensures proper partitioning during mitosis (McBride, 2013). This attachment is essential for the transition from transient to stable maintenance replication. E2 binds to specific sites near ori and to host mitotic chromosomes, facilitating the viral genome partitioning into daughter cells (Oliveira *et al.*, 2006). Additionally, E2 has been implicated in the regulation of cellular gene expression, growth inhibition, apoptosis, post-transcriptional RNA processing, and packaging of viral DNA (Johansson *et al.*, 2012; McBride, 2013; Parish *et al.*, 2006; Zhao *et al.*, 2000).

Structurally, E2 contains a transactivation domain and a DNA binding and dimerization domain (DBD), which are connected by a hinge region (McBride, 2013). The transactivation domain is approximately 200 amino acids long and is essential for transcriptional regulation, as well as for interaction with E1 and binding to host chromatin (Antson *et al.*, 2000; Chojnacki & Melendy, 2018; Kasukawa *et al.*, 1998; McBride, 2013; White *et al.*, 2003). The DBD, comprising 85-100 amino acids, mediates DNA sequence recognition and formation of stable E2 dimers (McBride *et al.*, 1988, 1989). The hinge region, although not well conserved

among HPVs, plays important roles in nuclear localization, chromatin binding, and interactions with host proteins (Lai *et al.*, 1999; McBride, 2013; Zou *et al.*, 2000).

In addition to the full-length E2 protein, some HPVs encode truncated E2 variants, including E8^E2, which retain the DBD but lack the transactivation domain (Kurg, 2011). These shorter forms function as negative regulators of viral transcription and replication by competing with full-length E2 for binding sites (Kurg, 2011; Lace *et al.*, 2008).

1.8 Existing systems for stable HPV replication investigation

Understanding stable beta HPV replication is essential for gaining insights into chronic infection mechanisms and developing targeted antiviral therapies. However, the development of reliable *in vitro* systems to study stable replication of beta HPV has been limited.

Primary keratinocytes, isolated from various body sites, such as foreskin, larynx, and cervix, are commonly used to study early HPV replication. These cells can support low-level replication of HPV genomes, and while they reflect the initial stages of infection, they have a limited lifespan, are costly to maintain, and are not suitable for long-term studies of stable episomal replication (Geimanen *et al.*, 2011; Kurg, 2011).

Cell lines derived from mild cervical dysplasia, such as W12 (HPV16) and CIN-612 (HPV31b), have been useful for studying alpha HPVs infections (De Geest *et al.*, 1993; Stanley *et al.*, 1989). They maintain episomal HPV genomes over multiple passages and have been used to study stable replication, episome loss, and viral integration (De Geest *et al.*, 1993; Pett *et al.*, 2004; Stanley *et al.*, 1989).

Recently, several keratinocyte-derived cell lines stably bearing episomal high-risk alpha HPV genomes have been described (Evans *et al.*, 2017; Sprague *et al.*, 2002). However, there are no comparable cell lines available for beta HPVs. Only one immortalized keratinocyte-derived cell line bearing an episomal beta-HPV49 genome has been described so far (Rehm *et al.*, 2022). This stable cell line was created due to the inactivation of the E8^E2 repressor and subsequent robust increase in HPV49-E8- genome copy numbers and E6/E7 expression levels that are required for proper immortalization (Rehm *et al.*, 2022).

The human osteosarcoma cell line U2OS has been widely used in HPV research. It supports replication of various circular HPV genomes, including beta HPVs, and allows for the

establishment of persistent HPV replication (Geimanen *et al.*, 2011). It is a promising platform for studying long-term HPV genome maintenance.

2 THE AIMS OF THE STUDY

In this study, we aimed to gain deeper insight into the roles of E1 and E2 viral proteins in stable HPV5 replication in U2OS cells. To achieve this, we:

- Designed and validated *E1* and *E2* targeting siRNAs
- Created a U2OS-based stable cell line bearing episomal HPV5-E1HA-Nluc-E2Flag genome, allowing for fast and efficient analysis of the genome copy numbers via measurement of Nluc activity and E1 and E2 protein detection using the epitope-specific antibodies
- Evaluated the *E1/E2* RNAi effects in stable replication of the wild-type (WT) and modified HPV5 genomes

3 EXPERIMENTAL PART

3.1 MATERIALS AND METHODS

3.1.1 DNA and siRNA constructs

- HPV5 m.c. — HPV5 WT genome (Sankovski *et al.*, 2014).
- HPV5-E1HA-Nluc-E2Flag m.c. — a modified HPV5 genome, where the HA tag-encoding sequence was inserted after the 15th nucleotide of the *E1* ORF, sequences encoding nanoluciferase and 2A region of foot-and-mouth disease virus were inserted after the *E1* stop codon, Flag tag-encoding sequence was introduced after the first ATG in the *E2* ORF (Lototskaja *et al.*, 2021).
- pLEX-Frb:Akt2-IRES-Hygromycin — Hygromycin resistance vector for mammalian cells (Addgene plasmid #120713), obtained from the molecular virology laboratory collection
- Scrambled siRNA control sense: UAGCGACUAAACACAUCAA, antisense: TAGCGACTAAACACATCAA (Sigma-Aldrich)
- HPV5 *E1* siRNA 1 sense: GUGGGAUAGGUGCAAUGUCAU, antisense: GTGGGATAGGTGCAATGTCAT
- HPV5 *E1* siRNA 2 sense: GGGCACUGGUCAGAUAUAGUA, antisense: GGGCACTGGTCAGATATAGTA
- HPV5 *E2* siRNA 1 sense: GAGCCAUGGACUCUAGUUGAU, antisense: GAGCCATGGACTCTAGTTGAT
- HPV5 *E2* siRNA 2 sense: GAGAAAGGUGUUACAAGGCUU, antisense: GAGAAAGGTGTTACAAGGCTT

All siRNAs contained dTdT overhang on their 3’ ends. Silencing RNAs were designed using the Invivogen siRNA Wizard web tool and produced by Microsynth AG, unless stated otherwise.

3.1.2 Cell lines

- Human osteosarcoma U2OS cell line (purchased from American Type Culture Collection (ATCC))

- Clone 15 stable cell line (Geimanen *et al.*, 2011) — U2OS-based cell line that maintains HPV5 m.c. in a stable manner
- Clone 14 stable cell line — U2OS-based cell line that maintains HPV5-E1HA-Nluc-E2Flag m.c. as an extrachromosomal plasmid. The cell line was created during this study.

3.1.3 Cell line handling and transfection

All cell lines were cultured in Iscove's Modified Dulbecco's Media (IMDM) (Corning), supplemented with 10% fetal calf serum (FCS) (Corning) and 1% penicillin/streptomycin (Sigma-Aldrich) at 37 °C in a humidified atmosphere containing 5% CO_2.

Cells were transfected via electroporation approximately 24 hours after splitting, using the Gene Pulser XCell system (Bio-Rad Laboratories) with the following settings: exponential mode, 220 V, 975 µF, in a 4 mm cuvette. For splitting, the medium was aspirated, and cells were washed with 3 ml of phosphate-buffered saline (PBS; 137 mM NaCl, 2.7 mM KCl, 8 mM Na_2HPO_4, and 2 mM KH_2PO_4) per 10 cm plate. Cells were then detached with 2 ml of 0.25% Trypsin-EDTA (Thermo Fisher Scientific) and plated onto new 10 cm plates with 10 ml of IMDM.

For transfections, a similar procedure was followed, except that cells were collected into Falcon tubes instead of being plated. Centrifugation was performed at 1000 rpm for 5 min in an Eppendorf Centrifuge 5810R (Thermo Fisher Scientific). After centrifugation, the medium was aspirated, and the cell pellet was resuspended in 250 µl of IMDM per transfection.

The following quantities of nucleic acids were used per 10 cm plate of confluent cells:

- 1.6–1.8 µg of HPV5-E1HA-Nluc-E2Flag m.c. or HPV5 w.t. m.c.
- 80 nM of *E1* siRNAs
- 40 nM of *E2* siRNAs
- 40 nM of scrambled control siRNAs

Additionally, 5 µg of salmon sperm DNA was used as carrier DNA for each transfection. The mixture of viral genome (if applicable), siRNAs (if applicable), and carrier DNA was added to 250 µl of cell suspension and transferred into an electroporation cuvette. After

electroporation, cells were transferred into fresh IMDM and plated according to the experimental needs.

3.1.4 Stable cell line generation and selection

3.1.4.1 Hygromycin B minimum lethal concentration determination

Based on a literature search (Dellal *et al.*, 2020; Munoz *et al.*, 2014) and antibiotic manufacturer protocol, U2OS cell viability testing was performed using the following concentrations of Hygromycin B Gold (InvivoGen): 50 µg/ml, 75 µg/ml, 100 µg/ml, 125 µg/ml, 150 µg/ml, 175 µg/ml, 200 µg/ml, and 250 µg/ml. The antibiotic solution was prepared in a cell-culturing medium. U2OS cells were plated at approximately 20-25% confluency on 24-well plates. Twenty-four hours after plating, the medium was changed to IMDM containing Hygromycin B at different concentrations. The medium was then replaced with fresh Hygromycin-containing IMDM every 3-4 days to maintain selection pressure. The effects on cell viability were evaluated by observing the cells under a light microscope at 10X magnification. Following a 7-day period of selection, it was established that the minimal lethal concentration of Hygromycin B Gold for U2OS cells was 175 µg/ml.

3.1.4.2 Generation of HPV5-E1HA-Nluc-E2Flag-positive clones

One 10 cm plate of U2OS cells was transfected with 1.8 µg of HPV5-E1HA-Nluc-E2Flag m.c. genome and 200 ng of Hygromycin B resistance gene expression vector in a ratio of 9:1 to ensure the presence of the HPV5-E1HA-Nluc-E2Flag genome in Hygromycin B-resistant cells. Transfected cells were seeded onto one 10 cm plate. Once confluent, cells were split onto eight 10 cm plates to ensure low density. The next day, the antibiotic-containing medium was added. Hygromycin B at a concentration of 175 µg/ml was used for the selection of positive clones.

Once colonies were visible, cells were washed with 1x PBS, single colonies were detached and resuspended in a drop of trypsin-EDTA and transferred onto 24-well plates using one colony per well.

Selected colonies were further propagated. Early during passaging, levels of HPV5-E1HA-Nluc-E2Flag genome replication in each clone were analyzed through Nluc assay, and only clones with Nluc levels comparable with Nluc activity typically observed in the transient system were further propagated.

3.1.5 Low molecular weight DNA isolation (Hirt method)

To isolate LMW DNA, 800 µl of Hirt lysis buffer (0.5% SDS, 50 mM Tris, pH 8.0, and 10 mM EDTA in water) was added to one 10 cm plate, previously washed with PBS, and incubated for 5 to 15 min at room temperature (RT). Following incubation, lysates were collected into the microtubes, and 200 µl of 5 M NaCl was added dropwise. Gentle end-to-end mixing was performed, followed by incubation at 4 °C overnight. Next day, lysates were centrifuged at 4 ℃ 14800 rpm for 15 min (Fresco 21 Microcentrifuge, Thermo Fisher Scientific). Then, supernatants were transferred to new microtubes, and 600 µl of isopropanol was added. The mixture was vortexed and incubated at -20 °C for at least 30 min or overnight. Afterward, the samples were centrifuged again for 15 min as previously described, the supernatant was removed, and DNA was resuspended in 200 µl of Sol IV buffer (20 mM Tris 7.5 pH, 100 mM NaCl, 10 µM EDTA, 0.2% SDS) supplemented with 50 µg/ml of Proteinase K, and incubated for 0.5-1 h at 56 °C. Then, 200 µl of phenol-chloroform (1:1) mixture (Sigma-Aldrich) was added, and samples were vortexed, followed by centrifugation at RT and 13000 rpm for 3 min (Heraeus Biofuge Pico, Heraeus instruments). The majority of the upper aqueous phase containing DNA was transferred to a new 1.5 ml microtube, and 450 µl of 96% ethanol was added to each sample for DNA precipitation. Samples were then vortexed and centrifuged at 4 ℃ and 14800 rpm for 15 min. The precipitates were then washed with 200 µl of ice-cold 75% ethanol and air-dried. Then, DNA precipitate was resuspended in 30 µl of TE buffer (MACHEREY-NAGEL) containing 20 µg/ml of RNase A (Thermo Fisher Scientific) and incubated at 37 °C for 1 hour. DNA concentrations were measured using a Nanodrop-1000 spectrophotometer (Thermo Fisher Scientific).

3.1.6 Southern blot and hybridization

LMW DNA was digested with restriction enzymes suitable for experimental goals. DpnI was used to digest bacterially input DNA in case of transient replication; SacI, BstxI, and BglI were used for the linearization of viral genomes; NheI and XbaI were used for the analysis of the uncut WT HPV5 and HPV5E1HANlucE2Flag, respectively. Approximately 16-20 µg of LMW DNA was used to analyze a pattern of the uncut viral genomes, and approximately 4-6 µg of LMW DNA was digested to visualize the linearized viral DNA. Additionally, 150 pg of linearized viral genome was used as a marker (M), and 3-4 ng of uncut viral genome was used for linearized and uncut gels, respectively. For restriction analysis, the LMW DNA was

digested with 1-2 µl of restriction enzyme (Thermo Fisher Scientific) in 30 µl of 1x FastDigest Green Buffer (Thermo Fisher Scientific) at 37 °C overnight.

After restriction, samples and 3-4 µl of GeneRuler 1 kb DNA Ladder (Thermo Fisher Scientific) were loaded onto 0.6-0.8% agarose-TAE (40 mM Tris-acetate, 1 mM EDTA) gel containing 30 µg of ethidium bromide (Invitrogen) per 100 ml. The gels were run at 40 V overnight.

The next day, the equal loading of DNA was visualized under the UV lamp. Then, gels were trimmed according to the regions of interest. Gels were first incubated in 0.25 M HCL for 10 min, followed by incubation in Solution A (0.5 M NaOH, 1.5 M NaCl) for 40 min, and Solution B (1 M Tris pH 8.0, 1.5 M NaCl) for 30 min. Then, the transfer sandwich was assembled according to **Figure 5**, using a charged nylon membrane (GSV). DNA transfer was performed overnight at RT in 10x SSC transfer buffer. After the transfer, the DNA was crosslinked to the air-dried membrane using Stratalinker UV crosslinker 1800 (Stratagene) for approximately 40 sec.

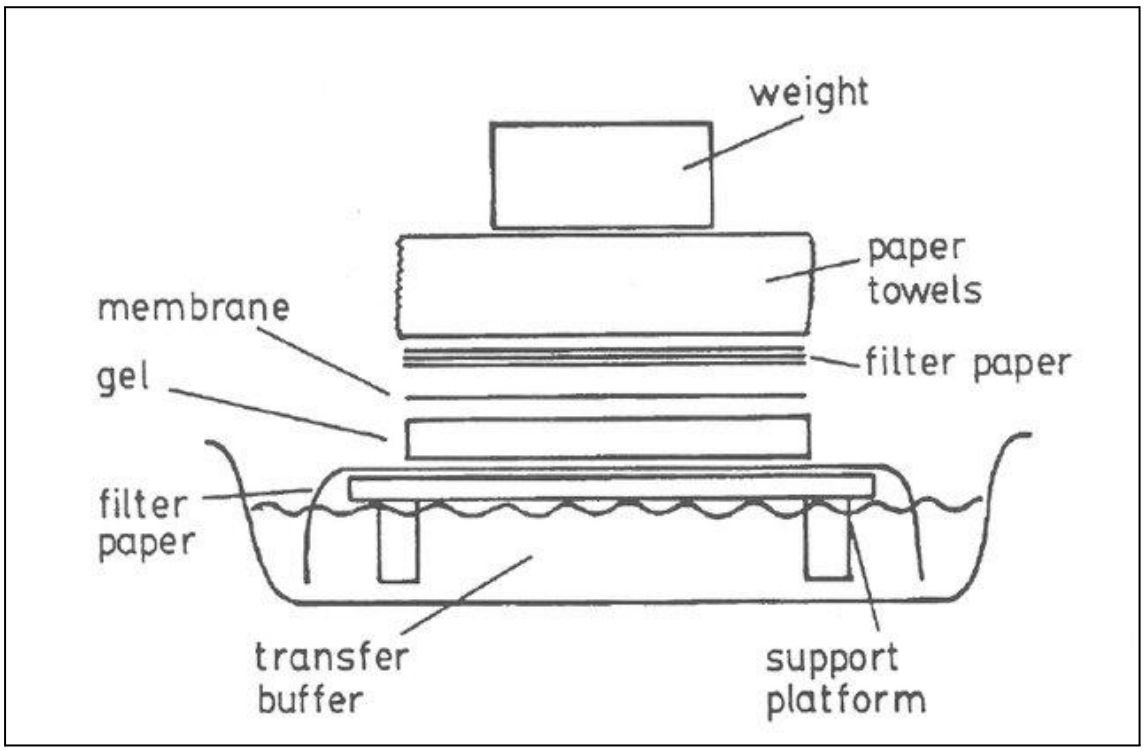

Figure 5. Southern blot transfer setup (Karcher, 1991).

The membrane was blocked in prehybridization solution (6x SSC, 5x Denhardt's Solution (1% Bovine serum albumin, 1% Ficoll, 1% Polyvinylpyrrolidone), 0.5% SDS, 0.2 mg/ml

denatured Salmon Sperm DNA in water) for an hour at 65 °C on rotation in the hybridization oven (GFL, 7601). In the meantime, the hybridization probe was synthesized. Random priming premix (0.2 µg of hexamer primer mix in 2.5x reaction buffer for Klenow Fragment (Thermo Fisher Scientific)) was mixed with 150 ng of linearized HPV5 m.c. DNA, and pure water was added up to 40 µl. The mixture was then denatured at 100 °C for 5 min, and chilled on ice. After the addition of 3 µl of 10 mM dNTPs mix without dATP (Thermo Fisher Scientific), 3 µCi of α-P33-dATP isotope (Hartmann Analytic), and 5 U of Exo-Klenow DNA polymerase (Thermo Fisher Scientific), the mixture was incubated at 37 °C for 15 min to start the synthesis of the new radioactively labelled DNA strand. Afterward, 4 µl of 10 mM dNTP mix was added, and the mixture was incubated at 37 °C for 15 min to finish the strand synthesis. Finally, the probe was denatured at 100 °C for 5 min and added to the membrane in the prehybridization solution. The membrane was incubated at 68 °C under rotation overnight.

The next day, the solution was discarded, and the membrane was washed in preheated washing solutions: SolI (2x SSC, 0.1% SDS) twice for 5 min, SolII (1x SSC, 0.1% SDS) once for 15 min, SolII (0.1x SSC, 0.1% SDS) twice for 10 min. After the washing step, the membrane was air-dried, placed in a transparent plastic folder, and exposed to a pre-cleared screen in a phosphoimager cassette (GE Healthcare Biosciences) for 24-72 h. The screen was scanned using an Amersham Typhoon Biomolecular Imager (GE Healthcare Biosciences) with a phosphor imaging plate to detect P33 radioisotope signals.

3.1.7 Luciferase assay

Cells were grown on 96-well plates in quadruplicate after transfection and washed twice with PBS prior to luciferase assay. The cells were lysed in 30 µl of 1x Luciferase Cell Culture Lysis Reagent (Promega) at RT on a shaker for 15 min. Then, 12 µl of cell lysate was transferred onto a white 96-well plate and mixed with 25 µl of Nano-Glo Luciferase Assay Substrate in 1x Luciferase Assay buffer (1:400, Promega). Chemiluminescence was measured using the GloMax 96 Microplate Luminometer (Promega). Alkaline phosphatase (AP) was used to normalize Nluc measurements. For AP measurement, 12 µl of cell lysate was mixed with 30 µl of Tropix CSPD Ready-To-Use Substrate (Thermo Fisher Scientific) on a white plate and incubated for 7 min prior to chemiluminescence measurement. RLU values were calculated by dividing Nluc values by AP values, afterward, the average of replicates, standard deviation, and p-values were calculated. All calculations were performed in

Microsoft Excel, and the results were plotted using the ggplot2 library in R, with error bars corresponding to one standard deviation.

3.1.8 RNA extraction

Cells were grown on 6 cm plates and washed with PBS prior to RNA extraction. Total RNA was isolated using the Quick-RNA Miniprep kit (Zymo Research). Cells were lysed with 600 µl of RNA lysis buffer. The lysate was then scraped using a cell scraper and transferred onto a yellow Spin-Away column in a collection tube. Centrifugation was performed at 13000 rpm for 1 min to remove genomic DNA. The flowthrough was collected, and 600 µl of ethanol was added and mixed thoroughly. The mixture was loaded onto a green Zymo-spin column, and the lysate was centrifuged at 13000 rpm for 30 seconds, and the flow-through was discarded. Next, 400 µl of RNA Prep Buffer was added to the column, followed by centrifugation at 13000 rpm for 30 seconds and discarding the flowthrough. Next, 700 µl of RNA Wash Buffer was applied, and the column was centrifuged at 13000 rpm for 30 seconds. After discarding the flowthrough, 400 µl of RNA Wash Buffer was added, and the column was dried via centrifugation at 13000 rpm for 2 min. Finally, RNA was eluted by adding 30 µl of nuclease-free water and centrifuging for 1 min. The concentration of eluted nucleic acids was measured using a Nanodrop-1000 spectrophotometer, and the extracts were stored at -70 °C until further use.

Approximately 7 µg of total RNA was treated with 3 µl of TurboDNase (Invitrogen) in 50 µl of 1x TurboDNase buffer (Invitrogen) for 2 hours at 37 °C to remove traces of genomic, viral, and carrier DNA. Following incubation, DNase was inactivated by incubation at 75 °C for 10 min in the presence of 15 mM EDTA. Next, RNA was precipitated by adding 32.5 µl of 7 M LiCl/15 mM EDTA, followed by incubation at -20 °C for at least 30 min and centrifugation at 4°C at 13000 rpm for 20 min. The supernatant was discarded, and 100 µl of RNA-grade 70% ethanol was added, the samples were then centrifuged for 4 min. After removing the ethanol, the pellet was air-dried and subsequently dissolved in 11 µl of nuclease-free water. The concentration of RNA was measured, and the samples were stored at -70 °C until further use.

3.1.9 Complementary DNA (cDNA) synthesis

Oligo(dT)-primed cDNA synthesis was performed using approximately 3 µg of total RNA and a RevertAid First Strand cDNA synthesis kit (Thermo Fisher Scientific). First, the total

RNA volume was adjusted to 11 µl with nuclease-free water. For each reaction, 1 µl of 100 µM oligo(dT) primer was added, and then the mixture was incubated at 65 ℃ for 5 min and placed on ice after a brief spin. For each reverse transcription reaction, 4 µl of 5x reaction buffer, 2 µl of 10 mM dNTP mix, 20 U Ribolock RNase Inhibitor enzyme, and 200 U of Reverse Transcriptase were added. For negative controls, validating the absence of traces of viral DNA, 1 µl of water was added instead of the Reverse Transcriptase. The tubes were then incubated at 42 ℃ for 1 hour, followed by heat inactivation of the enzymes at 70 ℃ for 5 min. All cDNA samples were stored at -20 ℃ until further use.

3.1.10 Quantitative polymerase chain reaction (qPCR)

The qPCR mix had the following composition: 1 µl of cDNA or 500 pg of LMW DNA, 1 µl of 10 µM oligonucleotide mix, 2 µl of 5x HOT FIREPol EvaGreen qPCR Mix Plus (Solis Biodyne), and 6 µl of water. Viral gene expression levels were measured in triplicate, and GAPDH or rDNA housekeeping gene levels were used to normalize them. Prior to the program run, the 384-well qPCR plate (Roche Diagnostics) was sealed and centrifuged at 1000 rpm for 2 min. The reactions were run using the LightCycler 480 II (Roche Diagnostics) machine according to the settings listed in **Table 3**. Afterward, absolute quantification analysis using the second derivative maximum method was performed through LighCycler software in order to quantify the cycle number at which the fluorescent signal crosses the threshold (CT values), further calculations were performed in Microsoft Excel, and the results were plotted using the ggplot2 library in R. Additionally, melting curves were visually assessed to confirm the absence of non-specific signals.

During further calculations, an average of triplicates was taken for all samples and primer sets. Then, GAPDH or rDNA average values were subtracted from viral gene average values to normalize their expression levels. Afterward, negative siRNA samples were used as reference values in RNAi experiments, and final values were calculated as follows: $2^{(CT_{neg.siRNA} - CT_{E1/E2\ siRNA})}$. Error bars were based on one standard deviation, and p-values were calculated using Excel software based on the results of multiple experiments.

Table 3. Quantitative PCR program for LightCycler 480 II. The continuous acquisition mode of melting curve operation means that fluorescence data is acquired continuously, and temperature is increased at a constant rate of 0.11 ℃/sec.

Operation		Temperature	Time	Number of cycles	Analysis mode
Preincubation		95 ℃	12 min	1	None
Amplification	Denaturation	95 ℃	15 sec	45	Quantification
	Annealing	58 ℃	15 sec		
	Extension	72 ℃	20 sec		
Melting curve		95 ℃	5 sec	1	Melting curve
		65 ℃	1 min		
		97 ℃	Continuous Acquisition (0.11 ℃/sec)		
Cooling		40 ℃	30 sec	1	None

3.1.11 Protein extraction and immunoprecipitation (IP)

Cells were grown on 10 cm plates until 70-90% confluency prior to lysis; 1 ml of cold RIPA lysis buffer ((50 mM Tris pH 7.5, 150 mM NaCl, 2 mM EDTA, 0.1% SDS and 0.1% TRITON-X100), supplemented with protease inhibitor cocktail (Roche)) was used per plate. The cell lysate was collected into 1.5 ml microtubes and further homogenized using a 26 G syringe, followed by incubation at 4 °C on slow end-to-end rotation for 40-60 min. The mixture was then centrifuged at 13000 rpm for 5 min at 4 °C in the Refrigerated Centrifuge 5810R (Eppendorf). E2 and E1 immunoprecipitation was carried out using 650 and 330 µl of supernatant, respectively. The remaining cell lysate (approximately 20 ul) was used for GAPDH immunoblotting.

The proteins were precipitated with Dynabeads Protein G (Thermofisher Scientific), which were conjugated with either an anti-E2 antibody (Lototskaja *et al.*, 2023) or an anti-HA tag antibody (Piirsoo *et al.*, 2019) produced in rabbit.

For immunoprecipitation, 3 µl of Dynabeads Protein G per sample was used. Beads were first washed with 1 ml of PBS, then with 1 ml of RIPA buffer. A magnet rack was used for precipitation. Afterward, the beads were resuspended in 100 µl per sample of RIPA buffer, approximately 2 µg per sample of the corresponding antibodies were added, and the mixture was incubated at RT for 30 min.

After the addition of the Dynabeads-antibody complexes, the samples were incubated at 4 °C on slow end-to-end rotation overnight. The following day, samples were precipitated on the magnet rack, and the pellet was washed twice with RIPA lysis buffer and resuspended in 20 µl of RIPA buffer.

3.1.12 Western blot

Following immunoprecipitation, 10 µl of 3x Laemmli buffer (62.5 mM Tris-HCl pH 6.8, 10% glycerol, 1% LDS, 0.005% Bromophenol Blue) containing 330 mM DTT was added to the 20 µl of protein samples, followed by 5-7 min of denaturation at 100 °C. Then, the samples were spun down and loaded onto the acrylamide gels. GAPDH samples were separated on a 12% gel, and 10% gels were used for E1 and E2.

The separating and stacking gel solutions were prepared according to **Table 4**. First, the separating gel mixture was poured into the assembled gel chamber (Bio-Rad) and topped with 1 ml of 96% ethanol to prevent air bubble formation. Once the separating gel hardened, ethanol was poured out, and the stacking mixture was prepared and poured on top, followed by the insertion of a gel comb. Prior to loading the samples, the comb was removed, and wells were washed with 1x SDS running buffer using a 16G syringe. 18 µl of denatured samples were loaded onto the gel, and 4 µl of PageRuler Prestained Protein Ladder (Thermo Fisher Scientific) was used.

The gels were run at a constant 23 mA/gel in the gel bath filled with 1x SDS until the desired separation of the ladder bands was achieved. For the wet transfer method, the PVDF membrane (Thermo Fisher Scientific) was briefly wetted in 100% methanol and preincubated in the transfer buffer (14.4 g/l glycine, 3.5 g/l Tris, 5% ethanol in water) for approximately 5 min. The transfer sandwich was assembled as follows, from black to transparent supports: sponge layer, 2 pieces of 5x8 cm whatman paper, gel without stacking part, PVDF membrane, 2 pieces of whatman paper, sponge layer. The transfer was performed at 400 mA for 1.5 hours using 1 l of cold transfer buffer and an ice pack to prevent overheating.

Table 4. Components for preparing separating and stacking gels. Components should be added in the order listed below, with ammonium persulfate and TEMED being last to avoid premature hardening.

Gel type (volume)	Component	Volume (ml)
10% separation gel (5 ml)	water	1.9
	30% acrylamide/bis solution, 37.5:1 (SERVA Electrophoresis GmbH)	1.7
	1.5 M Tris buffer (pH 8.8)	1.3
	10% SDS	0.05
	10% ammonium persulfate	0.05
	1,2-di-(dimethylamino)ethane (TEMED) (Thermo Fisher Scientific)	0.002
12% separation gel (5 ml)	water	1.6
	30% acrylamide/bis solution	2.0
	1.5 M Tris buffer (pH 8.8)	1.3
	10% SDS	0.05
	10% ammonium persulfate	0.05
	TEMED	0.002
Stacking gel (1 ml)	water	0.68
	30% acrylamide/bis solution	0.17
	1.0 M Tris buffer (pH 6.8)	0.13
	10% SDS	0.01
	10% ammonium persulfate	0.01
	TEMED	0.001

Following the transfer, the membrane was blocked in 5% non-fat dry milk solution in PBS containing 0.1% Tween (PBS-T) for 1 hour at room temperature. Then, the membrane was incubated with a primary antibody diluted in PBS-T solution containing 2.5% milk overnight at 4 °C. The following antibodies were used for different proteins: E1 - anti-HA-HRP 1:2000 (Sigma-Aldrich); E2 - anti-E2-rabbit 1:2000 (Icosagen); GAPDH - anti-GAPDH-HRP 1:7000

(Invitrogen). The next day, the membrane was washed with PBS-T for 15 min 3 times. For detection of the E2 protein, incubation with a secondary antibody for 40 min at RT was performed, using the goat-anti-rabbit-HRP diluted 1:10000 in PBS-T containing 2.5% non-fat dry milk. This was followed by the repetition of the washing step.

SuperSignal West Dura Extended Duration Substrate kit (Pierce) was used for exposure and HRP signal detection. Enhance and luminol solutions were mixed in a ratio 1:1 to a final volume of 800 µl and carefully distributed over the membrane. After a one-minute incubation, the membrane was washed in the PBS-T solution and placed into a film cassette. In the dark room, X-ray film (Agfa-Gevaert N.V.) was used for chemiluminescent signal detection and then developed for 50 sec and fixed for 30 sec in Developer and Fixer solutions (Agfa-Gevaert N.V.). Images were processed using Adobe Photoshop software.

3.1.13 Cell viability assay

The U2OS cell viability and proliferation were evaluated using CellTiter 96 AQ_{ueous} One Solution Cell Proliferation Assay (MTS) (Promega Corporation). This assay quantifies cell metabolic activity as an indicator of cell viability and number.

The same number of cells was transfected with different siRNAs and seeded onto transparent 96-well cell culture-grade plates in quadruplicate. Two days post-transfection, the medium was aspirated, and 90 µl per well of fresh IMDM was added using a multichannel pipette, followed by the addition of 18 µl per well of CellTiter 96 AQ_{ueous} One Solution Reagent. The plates were then incubated at 37 ℃ and 5% CO2 in a humidified atmosphere for 1-4 hours. Then, absorbance was measured at 490 nm using a Synergy H1 Multimode 96-well plate reader (Agilent BioTek). The averages and standard deviations of the quadruplicates were calculated using Microsoft Excel, and the results were plotted using the ggplot2 library in R.

3.1.14 Cell cycle analysis through flow cytometry

Cells were grown on 6 cm plates, detached using trypsin-EDTA, harvested into a 15 ml Falcon tube, and washed once with 1x PBS. The cell pellet was resuspended in 100 µl of PBS, and fixation was performed by adding 900 µl of cold 80% ethanol dropwise to the cell suspension while vortexing to minimize clumping and ensure even fixation. The mixture was incubated on ice for at least 30 min, followed by centrifugation at 300 g for 5 min and two washes with 1 ml of PBS. The cells were transferred to microtubes and centrifuged again

under the same conditions. The cell pellet was then resuspended in 500 µl of PBS, containing 5 µg of RNase A (Thermo Fisher Scientific) and 20 µg of propidium iodide (PI) (Sigma-Aldrich). The suspension was thoroughly mixed to ensure proper staining and incubated for 40 min in the dark at RT. Measurements were performed using the Attune NxT Flow Cytometer (Thermo Fisher Scientific). The flow cytometer laser was set at 488 nm wavelength, and the detection filter of 610/20 nm bandpass was used for PI detection. The event count was set between 5000 and 10000, depending on the density of cells used for the experiment. A uniform population of cells was selected using the control untreated U2OS cells sample, and the same thresholding was applied to other samples in the experiment. The size of cells and cell cycle phases were analyzed in the selected population and plotted using the Floreada.io online tool.

3.2 RESULTS

3.2.1 E1 and E2 RNAi inhibits the initial amplification of HPV5

To evaluate the effects of E1 and E2 on stable replication of HPV5 as a model for chronic infection, we applied RNAi using four different siRNAs, two targeting each gene.

First, we validated *E1* and *E2* silencing efficiency using RT-qPCR and Western Blotting, respectively. U2OS cells were co-transfected with the HPV5-E1HA-Nluc-E2Flag genome and the respective siRNAs, using a scrambled Neg.siRNA as a negative control. For mRNA quantification, total RNA was extracted 48 h post-transfection, and after cDNA synthesis, qPCR was performed using primers complementary to *E1* and *E2* sequences. GAPDH mRNA levels were used for normalization of *E1* and *E2* gene expression levels. For Western blottings, cells were lysed 72 h post-transfection, E1 and E2 were immunoprecipitated and detected using HA- and E2-specific antibodies, respectively. Additionally, we assessed whether RNAi had any effect on U2OS cell viability and proliferation. Cells were transfected with the corresponding siRNAs, and 48 h later, a viability assay was performed.

We observed a significant reduction in both transcript and protein levels for all *E1* and *E2* targeting siRNAs (**Figure 6B, C**). Furthermore, *E2* silencing led to a reduction in both *E1* mRNA transcript and protein levels. This result was expected considering the E2's role as a transcriptional activator of *E1* expression and the HPV5 transcription pattern, showing that in U2OS cells, the full-size *E1* is expressed only from transcripts that include *E2* (Sankovski *et*

al., 2014). Additionally, no statistically significant changes in U2OS cell viability and proliferation were detected (**Figure 6D**).

After validating siRNA efficiency, *E1* and *E2* silencing were analysed in a transient replication assay using HPV5-E1HA-Nluc-E2Flag genome and luciferase assay. It has been previously shown that HPV5-E1HA-Nluc-E2Flag genome copy numbers correlate with luciferase activity (Lototskaja *et al.*, 2021). The transient replication assay mimics the initial phase of viral genome replication, which is characterized by an increase in genome copy number to approximately 100–400 copies per infected cell. Nluc activity was measured 2, 3, and 4 days post-transfection and normalized to AP values, which indicate the number of viable cells in each sample. Compared to the control cells co-transfected with the viral genome and Neg.siRNA, a time-dependent decrease in luciferase activity was observed in the cells challenged with the *E1*- or *E2*-specific siRNAs, with average reductions of 1.5, 4.6, and 12.3-fold for 48 h, 72 h, and 96 h, respectively (**Figure 6A**). These data indicate that E1 and E2 are positive regulators of the initial phase of the HPV5 genome replication. Notably, the reduction was much more pronounced for *E2* targeting siRNAs, which could be attributed to the fact that Nluc and E2 proteins are expressed from the same viral transcript.

To further validate these findings, we performed a Southern blot analysis of the linearized viral DNA extracted from the U2OS cells transfected as described above, at different time points. A significant reduction in viral genome copy numbers compared to the Neg.siRNA control was observed in response to *E1* and *E2*-specific siRNAs (**Figure 6E**).

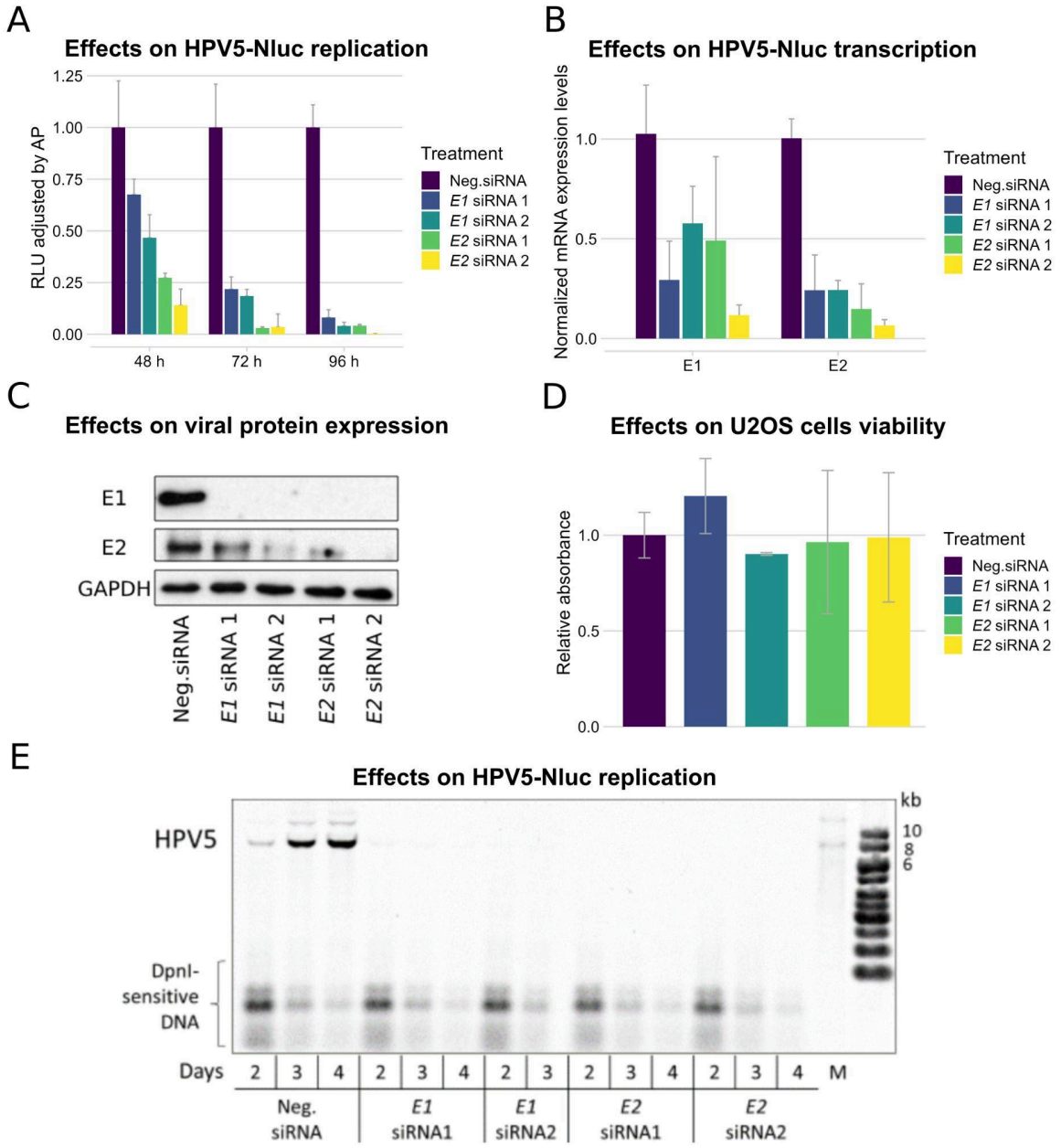

Figure 6. Validation of E1 and E2 siRNA efficiency in the transient replication assay in U2OS cells. Silencing effects on viral replication, transcription, and protein expression were analysed. For all experiments, U2OS cells were co-transfected with the HPV5-E1HA-NLuc-E2Flag genome and corresponding siRNAs, Neg.siRNA was used as a control, unless stated otherwise. (A) Luciferase activity was measured in quadruplicates at 48 h, 72 h, and 96 h post-transfection, and normalized to alkaline phosphatase activity. The normalized Nluc activity values for the control samples were set as 1 at every time point, data from other samples are presented relative to the control. The average means +/- SD of three independent experiments are presented. All differences between Neg.siRNA samples and

other samples were statistically significant (p-value < 0.05). (B) Levels of the *E1* and *E2* viral transcripts were measured in triplicate using RT-qPCR 72 h post-transfection. GAPDH mRNA expression levels were used for normalization. The normalized *E1* and *E2* mRNA expression levels in the control samples were set as 1, and data from other samples are presented relative to the control. The average means +/- SD of two independent experiments are presented. Differences in mRNA expression levels in samples co-transfected with *E1* and *E2* targeting siRNAs compared to control were statistically significant (p-value <0.05). (C) E1 and E2 proteins were immunoprecipitated and analyzed using Western blotting and HA- and E2-specific antibodies 72 h post-transfection. GAPDH was used as a loading control. (D) U2OS cells were transfected with *E1* and *E2* targeting siRNAs, and viability was measured 48 h post-transfection in technical triplicate. The number of viable cells in the samples transfected with the Neg.siRNA was taken as 1. No statistically significant differences between the negative control and siRNAs were observed. (E) U2OS cells were transfected as indicated, and total DNA was extracted at 48 h, 72 h, and 96 h post-transfection and analysed using Southern blotting. Six µg of DNA was digested with DpnI and SacI to cut the input DNA and linearize the viral genome, respectively. DNA was separated on a 0.8% agarose-TAE gel, and hybridized with the radioactively labelled viral genome. M corresponds to the linearized HPV5-E1HA-Nluc-E2Flag m.c. genome.

3.2.2 Establishment of the stable cell line bearing the episomal HPV5 genome

Next, to create a cellular model for persistent beta-HPV infection, we aimed to develop a stable U2OS-based cell line bearing the HPV5-E1HA-Nluc-E2Flag genome episomally. U2OS cells were transfected with the HPV5-E1HA-Nluc-E2Flag genome and a vector expressing the Hygromycin B resistance gene in a 9:1 proportion. After one round of passaging, antibiotic-containing medium was added to the cells to select the resistant clones. The individual colonies were picked up and propagated further separately. Seventeen clones were obtained following this subcloning protocol.

Luciferase activity was measured in each clone to assess the presence and copy number of the Nluc-positive viral genome. Only three clones, 10, 11, and 14, showed high levels of luciferase activity, which indicates the presence of high copy numbers of the Nluc-positive viral genome in these cells (**Figure 7A**). These clones were selected for further testing.

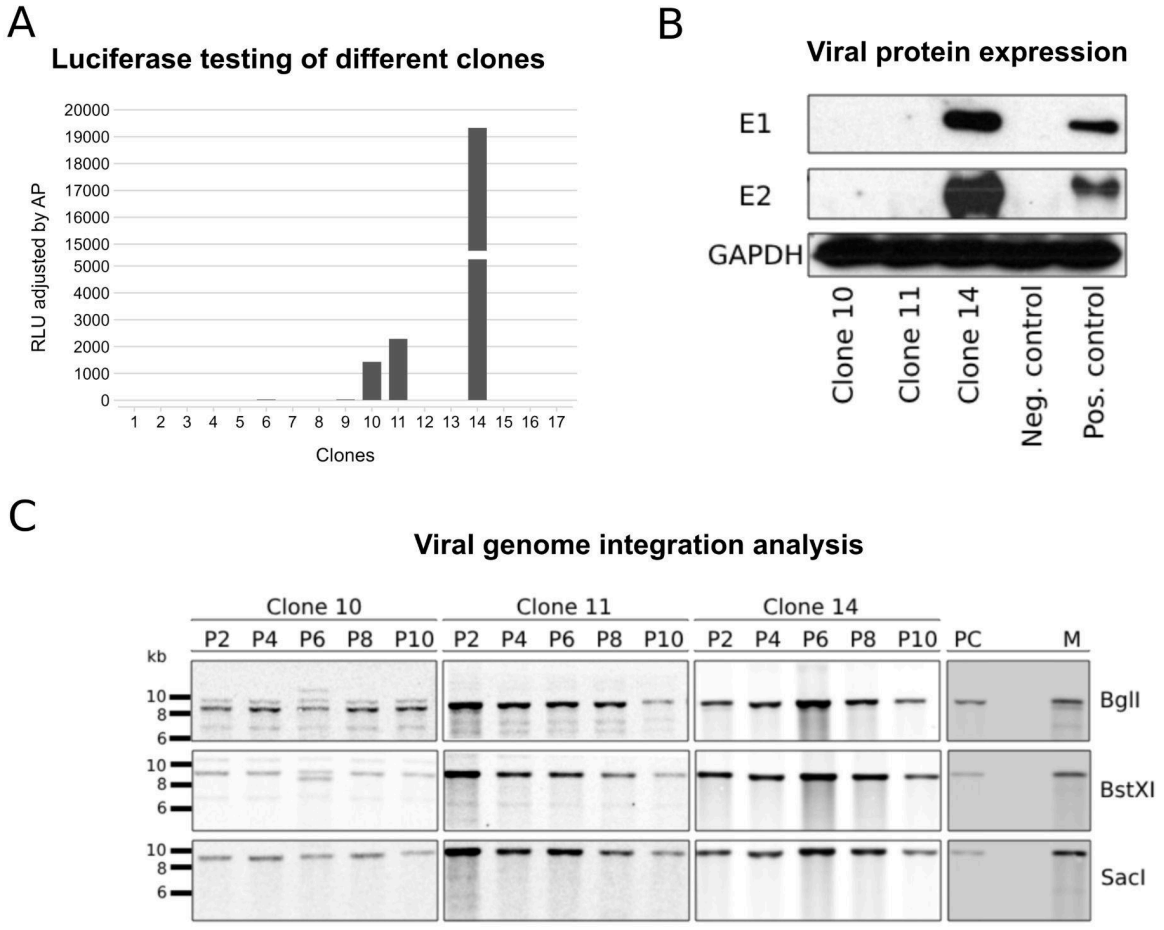

Figure 7. Characterisation of stable cell line clones. (A) To select the HPV5-E1HA-Nluc-E2Flag-positive cells, Nluc activity was measured and normalized to AP activity in 17 individual hygromycin-resistant clones. The y-axis section between 5000 and 15000 relative light units (RLU) is omitted to improve readability. (B) Clones 10, 11, and 14 were grown on 10 cm plates. Immunoprecipitation followed by Western blotting was performed to analyse the E1 and E2 protein levels, GAPDH served as the loading control. Neg. and Pos. controls correspond to the lysates isolated from untransfected U2OS cells and U2OS transiently transfected with HPV5-E1HA-NLuc-E2Flag genome, respectively. (C) To assess the viral genome integration into the host cell genome, LMW DNA was extracted at various passages and linearized with BglI, BstXI, or SacI restriction enzymes. 6 µg of DNA was used per restriction, DNA was separated on a 0.8% agarose-TAE gel, and hybridized with the radioactively labelled viral genome. PC and M correspond to U2OS cells transfected with HPV5-E1HA-NLuc-E2Flag genome and HPV5-E1HA-NLuc-E2Flag m.c. treated with the same restriction enzymes used as a marker, respectively.

To evaluate whether the viral genome is expressed episomally or has integrated into the host cell genome, we performed Southern blot analysis of LMW DNA extracted from clones 10, 11, and 14, linearized using three different restriction enzymes, each of which cuts the HPV5-E1HA-NLuc-E2Flag genome at a unique site located far apart from each other — within L1, E2, and E7 genes, respectively (**Figure 7C**). In case of an episomal viral genome, digestion with a single-cutter enzyme will linearize HPV5-E1HA-NLuc-E2Flag genome, resulting in a single band of approximately 8.5 kb. Integration of a viral genome into the host chromosomes typically disrupts this pattern, as the viral genome often becomes fragmented or rearranged, resulting in irregular restriction pattern and the appearance of bands of unexpected sizes (see **Supplementary Figure 1**). We observed this for Clone 10 when cut with BglI or BstXI and for Clone 11 when cut with BglI, BstXI, or SacI. These results indicate that only Clone 14 bears the episomal HPV5-E1HA-NLuc-E2Flag genome, while other clones contain, along with the episomal copies, also the integrated viral genome.

Next, we evaluated the viral E1 and E2 protein expression in the three clones using immunoblotting (**Figure 7B**). U2OS cells transfected with the HPV5-E1HA-NLuc-E2Flag genome were used as a positive control. Expression of E1 and E2 proteins was below the detection level in clones 10 and 11, while clone 14 showed E1 and E2 expression levels higher than those of the transiently expressed HPV5-E1HA-NLuc-E2Flag genome (Pos. control on **Figure 7B**). Taken together, these data indicate successful creation of a monoclonal cell line bearing multiple copies of the episomal HPV5-E1HA-NLuc-E2Flag genome.

3.2.3 Characterization of HPV5-E1HA-NLuc-E2Flag and HPV5 WT-positive cell lines

After analyzing the integration status and viral protein expression levels in the selected clones, we proceeded with the propagation of the clone 14, hereafter referred to as H5-Nluc+, and compared it to a previously generated cell line bearing the HPV5 WT genome, hereafter referred to as H5+ cells (Geimanen *et al.*, 2011, clone 15).

First, we evaluated the viral genome integration status in H5+ cells using the same method as for previously generated clones in **Figure 7C**. Restriction analysis revealed no prominent bands of unexpected size, indicating that the viral genomes in H5+ cells are primarily

maintained episomally (**Figure 8A**). We then compared the cell cycle profiles, cell size, viral DNA oligomer patterns, and genome copy numbers between H5+ and H5-Nluc+ cells.

Cell cycle and size were assessed by flow cytometry using PI staining to determine whether stable maintenance of the viral genome had any adverse effects on cell division and growth. All cells were cultured on 10 cm plates. Initial gating was based on untransfected U2OS cells, which served as a control. No prominent differences were detected in cell cycle or cell size profiles. Representative results from one of two independent experiments are shown in **Figure 8B**.

The physical state of the viral genome DNAs was analyzed in both H5+ and H5-Nluc+ cells. Previous studies have shown that specific oligomers of HPV16, HPV18, and HPV11 DNA, which are absent during early viral replication, can replicate independently of E1 function in stable cell lines (Egawa *et al.*, 2012; Murakami *et al.*, 2019; Piirsoo *et al.*, 2020). Similarly, it has been previously suggested that replication of a certain oligomeric form of the viral genome in H5+ cells, commonly referred to as the dominant replicon (DR), can occur in an E2 activity-independent manner (Lototskaja *et al.*, 2021). Based on these findings, we aimed to analyse the physical state of the viral genomes in the stable cell lines and in the transiently transfected cells and compare it with the viral DNA genomes used for transfections.

For this analysis, LMW DNA was extracted from cells grown on 10 cm plates. For transient replication controls (PC), DNA was harvested three days post-transfection, for marker (M), 6 ng of the HPV5 m.c. genome was used. All samples were treated with a restriction enzyme to digest the host DNA, while leaving the viral genome uncut. The DNA samples were then separated on a 0.6% agarose-TAE gel and hybridized with a radioactively labelled viral genome probe.

In H5+ cells, we observed the previously described DR, the expression of which was negligible during transient replication of the HPV5 genome or in the input HPV5 DNA (PC and M on **Figure 8C**, respectively). In contrast, the oligomers pattern of the viral genome in the H5-Nluc+ cells largely resembled that of early viral replication (**Figure 8D, PC**), with the exception of an additional band, marked with an asterisk, observed in the two later passages. This band was undetectable during the transient replication of the same viral genome and may represent an early form of DR. Additionally, the DR has been reported to emerge after prolonged propagation of the cells maintaining the viral genome, as exemplified by the H5+

cell line generated more than 15 years ago (Geimanen *et al.*, 2011; Lototskaja *et al.*, 2021). In contrast, the H5-Nluc+ cell line was generated during this study, which might explain the absence of DR.

Additionally, viral genome copy numbers were quantified by qPCR using LMW DNA extracts from three different passages of each cell line and primers specific for the *E1* and *E2* genes. Viral genome copy numbers were normalized to those of ribosomal DNA. The first passage of H5+ cells was set as 1, and copy number values for H5-Nluc+ are presented relative to it. On average, the viral genome copy number was approximately 16-fold higher in H5-Nluc+ cells, generated in this study, compared to the H5+ clone (**Figure 8E**). This difference was statistically significant.

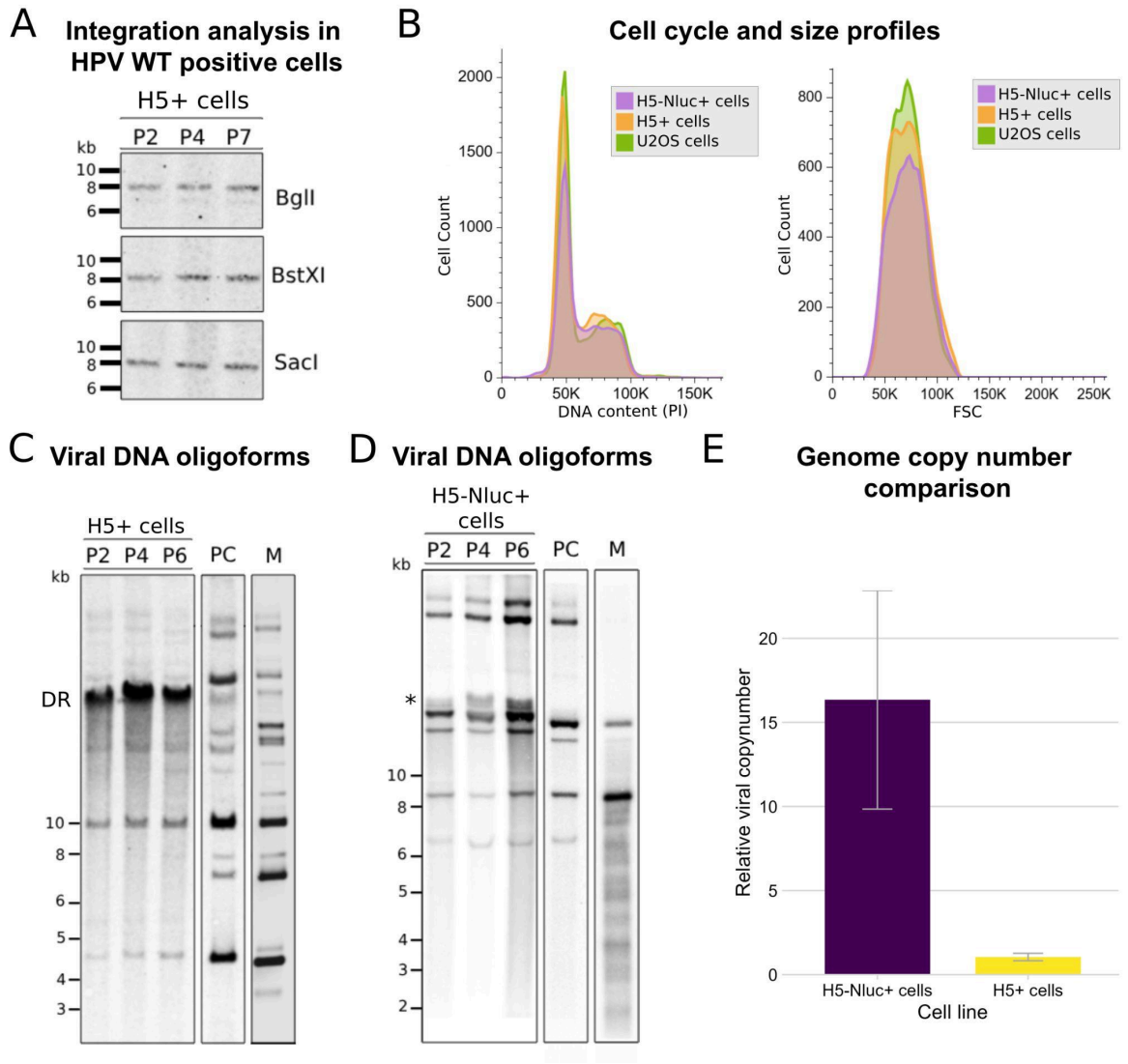

Figure 8. Characterization of the HPV5-E1HA-NLuc-E2Flag (H5-Nluc+ cells) and HPV5 WT-positive (H5+ cells) cell lines. (A) To assess viral genome integration in H5+

cells obtained from our laboratory collection, LMW DNA was extracted at different passages, and 6 µg of DNA was digested with BglI, BstXI, or SacI restriction enzymes. DNA was separated on a 0.8% agarose-TAE gel, transferred to a membrane, and hybridized with a radioactively labelled HPV5 genome. (B) Cell cycle profiles and size of H5+ and H5-Nluc+ cells were analyzed by flow cytometry following PI staining. U2OS cells were used to set the flow cytometry control parameters, including cell population gating, and cell cycle phases were assessed based on PI fluorescence relative to cell count, while cell size was evaluated using forward scatter area (FSC-A) signals. (C) To evaluate the physical state of the viral DNA in H5+ cells, LMW DNA was extracted at different passages. Approximately 20 µg of DNA per sample was treated with a restrictase that doesn't cut the viral genome, separated on a 0.6% agarose-TAE gel, and hybridized with the radioactively labelled viral genome. PC and M correspond to LMW DNA isolated from U2OS cells transfected with HPV5 WT genome and HPV5 WT m.c. DNA used as a marker, respectively. (D) The viral DNA isoforms in H5-Nluc+ cells were analyzed as described in panel C. PC and M correspond to LMW DNA from U2OS cells transfected with HPV5-E1HA-NLuc-E2Flag genome and HPV5-E1HA-NLuc-E2Flag m.c. DNA used as a marker, respectively. (E) Viral genome copy number was determined by qPCR using primers targeting the *E1* and *E2* genes. For each reaction, 500 pg of LMW DNA extracted from H5+ and H5-Nluc+ cells at three different passages was used. Ribosomal DNA expression levels were used for normalization. Gene expression levels in H5+ cells were set to 1, and values for H5-Nluc+ cells are presented relative to this. The average of *E1* and *E2* gene expression levels was used to estimate genome copy number. Differences between H5+ and H5-Nluc+ cells were statistically significant (p-value < 0.05).

3.2.4 E1 and E2-dependent stable replication of beta-HPV5

To investigate the role of E1 and E2 proteins in stable HPV5 genome maintenance, we silenced their expression in H5+ and H5-Nluc+ cells using RNAi and assessed the effects on replication of viral genomes and their specific oligomers. In H5-Nluc+ cells, we additionally evaluated genome replication through luciferase assay and measured viral protein expression levels.

To assess the effects of *E1* and *E2* silencing on stable replication of the HPV5 genome, H5+ and H5-Nluc+ cells were transfected with the respective siRNAs. LMW DNA was extracted at 3, 4, or 5 days post-transfection. The extracts were subsequently treated with a viral

genome single-cutter or a non-cutting restriction enzyme to generate linear or uncut viral DNA, respectively. The DNA samples were separated on 0.8% (linearized) or 0.6% (uncut) agarose-TAE gels and hybridized with a radioactively labelled HPV5 probe.

In H5+ cells, E1 and E2 silencing resulted in an average decrease of 24%, 45%, and 51% in linearized DNA signals at days 3, 4, and 5 post-transfection, respectively, compared to the negative control samples (**Figure 9A**, top panel). Additionally, we observed lower levels of most viral DNA oligomers in response to the *E1* and *E2* silencing, while replication of the DR remained largely unaffected (**Figure 9A**, bottom panel). These results suggest the presence of two replication mechanisms in H5+ cells: one dependent on E1 and E2, and another driven primarily by host cell replication machinery. Similar observations have been previously reported for HPV16, HPV18, and HPV11 (Egawa *et al.*, 2012; Murakami *et al.*, 2019; Piirsoo *et al.*, 2020).

In contrast, *E1* and *E2* silencing in H5-Nluc+ cells was approximately 20% more efficient, showing average reductions of 53% and 76% in linearized viral DNA levels at days 3 and 5, respectively, compared to the control samples (**Figure 9B**). Unlike H5+ cells, no clear pattern of specific oligomeric forms being differently affected by the *E1* or *E2* silencing was observed.

The silencing effects on stable replication of the H5-Nluc+ genome were additionally validated using a luciferase assay. The HPV5-Nluc+ cells were transfected with the E1/E2-specific or Neg. siRNAs. Luciferase activity was measured at 48, 72, and 96 h post-transfection and normalized by AP activity. Silencing of *E1* or *E2* resulted in an average 80% reduction in Nluc activity at 96 h post-transfection that correlates with the Southern blotting results (**Figure 9C**). The silencing efficiency was less pronounced at earlier time points, as the viral genome is actively replicating prior to siRNA treatment. Consequently, *E1* and *E2* silencing leads to a gradual decrease in viral DNA copy number over subsequent cell divisions. This contrasts with transient viral replication, where the viral genome is introduced simultaneously with the siRNAs, and *E1*/*E2* silencing occurs early in viral replication, resulting in more immediate and pronounced inhibition (**Figure 6A, Figure 9C**).

Finally, we examined E1 and E2 protein levels at 72 hours post-transfection using IP and western blotting with HA- and E2-specific antibodies. In H5-Nluc+ cells transfected with *E1* targeting siRNAs, E1 protein was undetectable, and E2 levels were severely reduced.

Conversely, transfection with *E2* targeting siRNAs led to a significant decrease in E1 expression and a partial reduction in E2 levels compared to the negative control (**Figure 9D**).

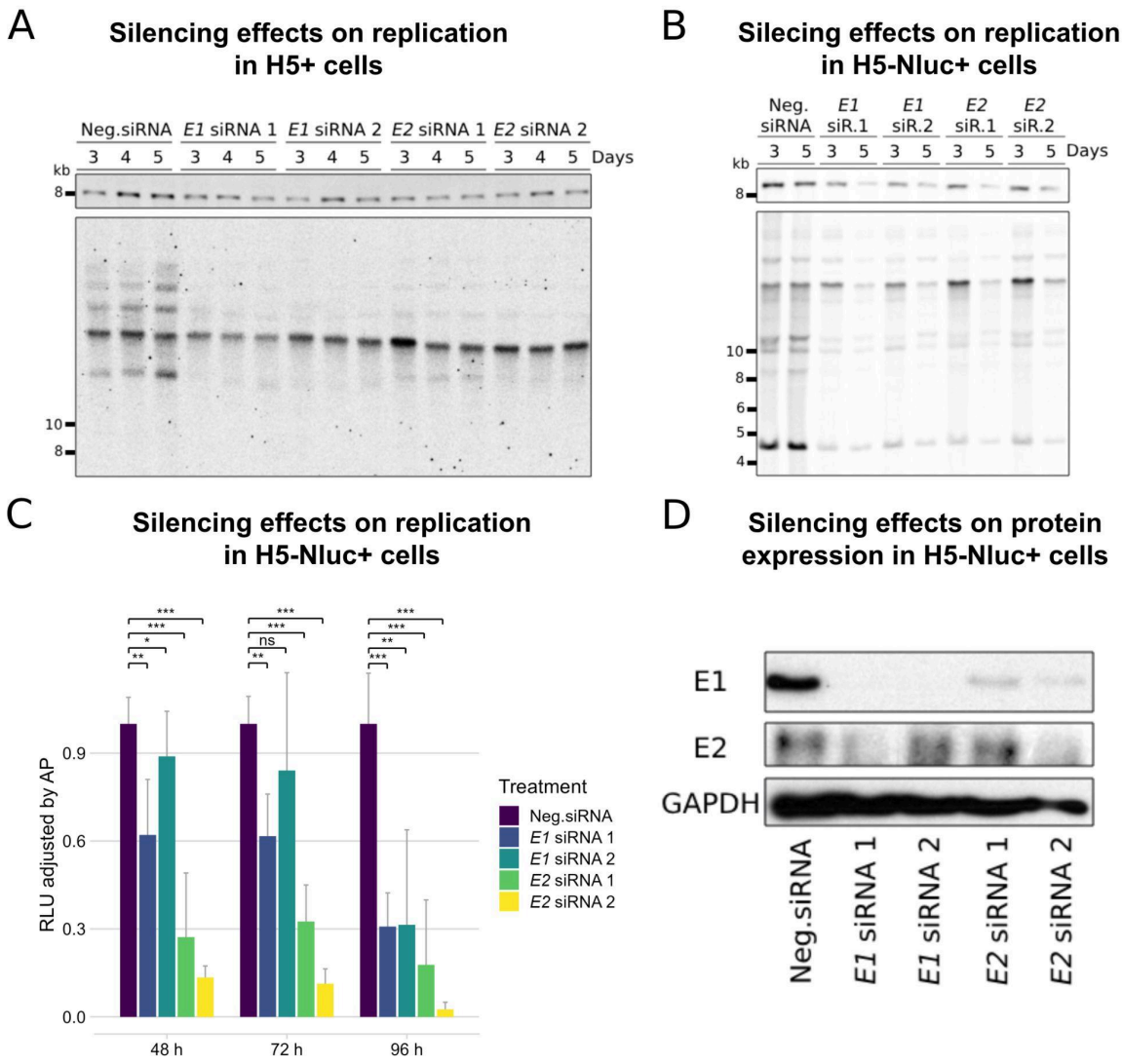

Figure 9. Effects of E1 and E2 silencing on stable replication of HPV5. The cells were transfected with the indicated siRNAs. (A-B) LMW DNA from H5+ or H5-Nluc+ cells was extracted at 3, 4, and 5 days post-transfection. Approximately 6 µg and 20 µg of DNA per sample were treated with either one-cutter or non-cutting restriction enzymes, separated on 0.8% or 0.6% agarose-TAE gel for the analysis of the linear and uncut viral DNA, respectively. The DNA was hybridized with the radioactively labelled HPV5 probe. The images showing linearized and uncut viral DNA are presented on the top and bottom panels, respectively. (C) The cells were seeded onto 96-well plates after transfection. Nluc activity was measured at 48, 72, and 96 h post-transfection, and normalized by AP. The normalized

RLU values for each time point are presented relative to that of cells transfected with the Neg.siRNA, which was taken as 1. Statistical significance is presented above the bars: p-value > 0.05 - ns, p-value < 0.05 - *, p-value < 0.01 - **, p-value < 0.001. (D) Silencing effects on E1 and E2 protein levels were analyzed through IP and western blotting with HA- and E2-specific antibodies 72 h after transfection with the corresponding siRNAs. GAPDH was used as a loading control.

4 DISCUSSION

Skin-infecting HPVs are associated with various lesions that may progress to cancer, particularly in immunocompromised individuals. Long-term maintenance of the viral genome within host cells—its replication in concert with the host DNA and transmission to daughter cells—is typically a prerequisite for cancer development. Currently, a limited understanding of the molecular mechanisms underlying stable replication of cutaneous HPVs hinders the development of new antivirals needed for cancer prevention and treatment.

One of the most promising directions for antiviral drug development against cutaneous HPVs is targeting the E1 and/or E2 viral proteins shown to be absolutely required for the initial phase of the viral genome replication in different cellular models. However, their role in the stable replication of cutaneous HPVs remains to be elucidated. The main obstacle for these studies is the absence of an appropriate cellular model.

In this study, we established and characterized a U2OS-derived cell line harboring the episomal HPV5E1HA-Nluc-E2Flag genome. This cell line was created to complement the previously described H5+ cell line bearing the WT HPV5 genome (Geimanen *et al.*, 2011). However, the new cell line enables easier monitoring of viral genome copy number through measurement of highly sensitive Nluc activity as well as detection of the HA-tagged E1 and Flag-tagged E2 viral proteins using the tag-specific antibodies. The viral genome copy number in H5-Nluc+ cells was considerably higher than that in H5+ cells, simplifying viral DNA and protein detection from a small number of cells, which may be a useful tool for high-throughput screening of antiviral drugs.

Analysis of the physical state of both extrachromosomal viral genomes revealed a pattern similar to that during transient replication of the same genomes in U2OS cells. Our data indicated that the monomeric forms of both viral genomes, as well as their oligomers, replicate in an E1/E2-dependent manner. However, comparative analyses of H5+ and H5-Nluc+ cells also revealed important differences in the maintenance of specific viral genome oligomeric forms, with H5-Nluc+ cells missing the oligomeric form replicating independently of the E1 and E2 proteins, which is present in H5+ cells as a dominant replicon comprising approximately 50% of the viral DNA.

At present, it is unknown whether this specific oligomeric form of viral DNA, which replicates in an E1/E2-independent manner, exists in keratinocytes during natural infection. If

this mode of replication exists in HPV natural host cells, targeting E1/E2-dependent HPV replication with antiviral drugs may be ineffective. However, to the best of our knowledge, no cellular models based on cutaneous HPV-positive keratinocytes are currently available. The oncogenic potential of cutaneous HPVs is relatively low compared to the mucosal types, and they are unable to immortalize primary keratinocytes or persist in host cells during long-term cultivation. So far, only one keratinocyte-derived immortalized cell line harboring an extrachromosomal beta-HPV49-E8- genome has been described (Rehm *et al.*, 2022). In this model, knockout of the *E8^E2* repressor led to high expression of the viral oncogenes E6 and E7, which in turn enabled immortalization of primary keratinocytes. Our study showed that HPV5-E1HA-Nluc-E2Flag genome copy numbers were substantially higher than those of the HPV5 WT genome in the corresponding U2OS-derived cell lines, suggesting that the HPV5-E1HA-Nluc-E2Flag genome may be a suitable candidate for successful keratinocyte immortalization.

In future studies, along with creating the immortalized HPV5-E1HA-Nluc-E2Flag-positive keratinocytes as a model for studying the stable cutaneous HPV replication, it would be valuable to test whether increasing the concentration of the used siRNAs or/and duration of the treatment through repeated transfections would lead to repression of the DR replication in H5+ cells and whether it could lead to a complete elimination of the viral genome in H5-Nluc+ cells. Additionally, investigating the effects of the multiple *E1*/*E2*-specific siRNA combinations may reveal more efficient strategies for inhibiting viral replication.

Our findings confirm that both E1 and E2 proteins are required for the HPV5 replication during the initial phase after transfection of the viral genome, but it remains unclear whether they are necessary for the long-term maintenance of viral replication.

SUMMARY

Cutaneous HPV can cause lesions that may progress to cancer, especially in immunocompromised patients. Long-term persistent viral genome replication is a key process associated with skin cancer. However, the molecular mechanisms of the HPV stable replication are poorly understood.

In this study, we aimed to investigate the role of the E1 and E2 proteins in the transient and stable modes of HPV5 replication. HPV5 was chosen as the best-studied cancer-associated cutaneous beta-HPV type. We analyzed the effects of *E1* and *E2* knockdown on the transient HPV5 replication, representing the initial phase of the replication cycle after infection of a host cell. Additionally, we generated a U2OS-derived cell line bearing the extrachromosomal HPV5-E1HA-Nluc-E2Flag genome (referred to as H5-Nluc+) to study stable HPV5 replication. The newly established cell line was compared to a previously described cell line carrying the HPV5 WT genome (H5+). We evaluated the impact of *E1* and *E2* silencing in both stable cell lines to better understand the role of these viral proteins in episomal maintenance.

This study resulted in the following conclusions:

- *E1* and *E2* targeting siRNAs can efficiently inhibit the expression of the corresponding viral transcripts
- E1 and E2 are essential for the establishment of HPV5 replication
- The established cell line bears the viral genome episomally and has a different pattern of oligomeric forms of viral DNA than that in H5+ cells
- Effects of *E1* and *E2* silencing in the H5+ cell line suggest that two modes of HPV5 stable replication exist, one dependent on E1 and E2 proteins and another reliant on host cell machinery
- These findings were not confirmed in H5-Nluc+ cells, suggesting that an E1 and E2-independent mode of replication develops after prolonged maintenance of viral replication

SUPPLEMENTARY MATERIALS

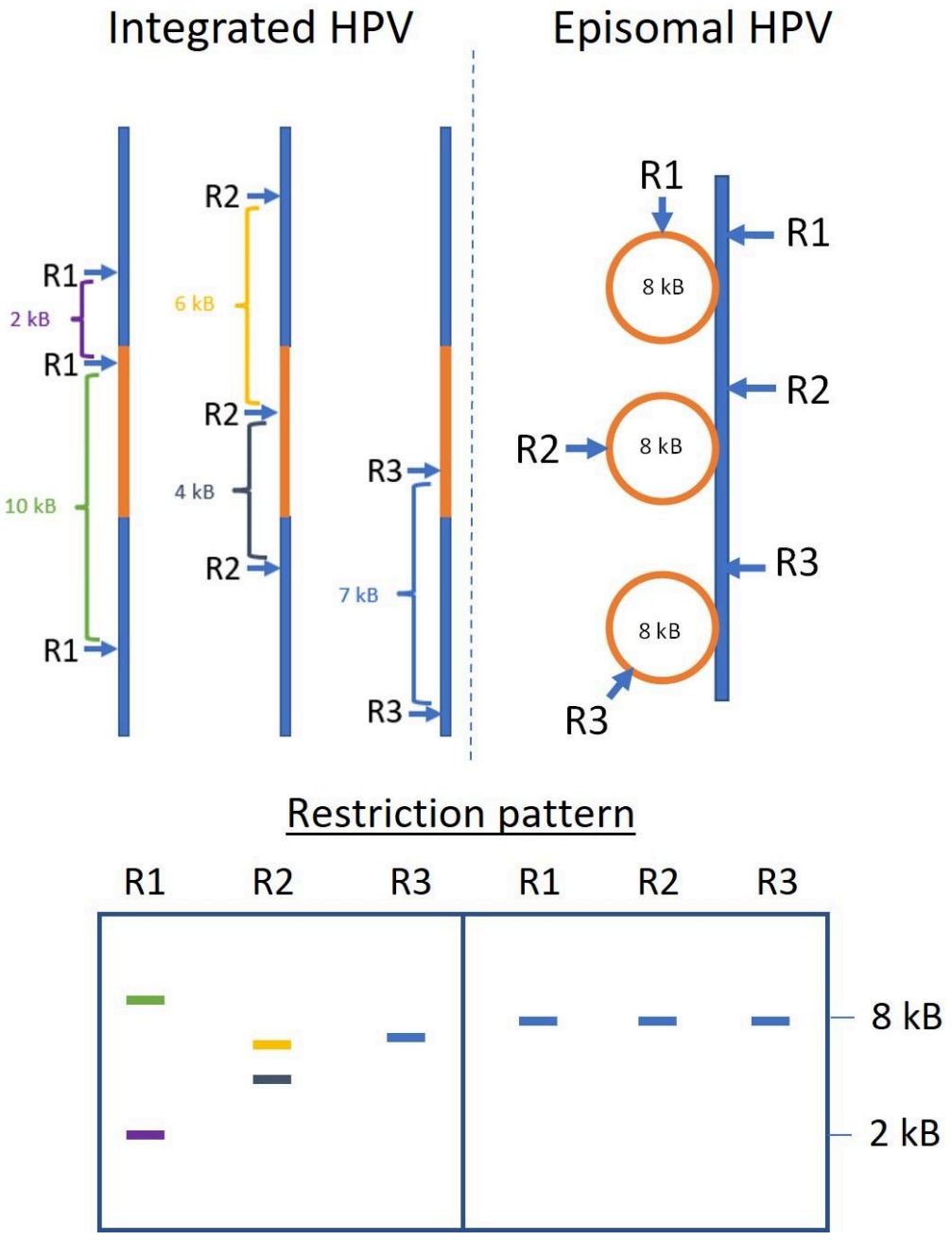

Supplementary Figure 1. Viral genome integration and restriction patterns on Southern blotting. The top panel illustrates viral genomes (orange) and host DNA (blue). Restriction enzymes are marked as R1, R2, and R3, with arrows indicating their specific sites. Curly brackets denote the expected restriction fragment size; their colors correspond to the band colors shown in the bottom panel.

REFERENCES

Antson, A. A., Burns, J. E., Moroz, O. V., Scott, D. J., Sanders, C. M., Bronstein, I. B., Dodson, G. G., Wilson, K. S., & Maitland, N. J. (2000). Structure of the intact transactivation domain of the human papillomavirus E2 protein. *Nature*, *403*(6771), 805–809. https://doi.org/10.1038/35001638

Arbyn, M., Sanjosé, S. de, Saraiya, M., Sideri, M., Palefsky, J., Lacey, C., Gillison, M., Bruni, L., Ronco, G., Wentzensen, N., Brotherton, J., Qiao, Y.-L., Denny, L., Bornstein, J., Abramowitz, L., Giuliano, A., Tommasino, M., & Monsonego, J. (2012). EUROGIN 2011 roadmap on prevention and treatment of HPV-related disease. *International Journal of Cancer*, *131*(9), 1969–1982. https://doi.org/10.1002/ijc.27650

Aydin, I., Villalonga-Planells, R., Greune, L., Bronnimann, M. P., Calton, C. M., Becker, M., Lai, K.-Y., Campos, S. K., Schmidt, M. A., & Schelhaas, M. (2017). A central region in the minor capsid protein of papillomaviruses facilitates viral genome tethering and membrane penetration for mitotic nuclear entry. *PLoS Pathogens*, *13*(5), e1006308. https://doi.org/10.1371/journal.ppat.1006308

Bergvall, M., Melendy, T., & Archambault, J. (2013). The E1 proteins. *Virology*, *445*(1), 35–56. https://doi.org/10.1016/j.virol.2013.07.020

Bruni, L., Diaz, M., Castellsagué, M., Ferrer, E., Bosch, F. X., & de Sanjosé, S. (2010). Cervical Human Papillomavirus Prevalence in 5 Continents: Meta-Analysis of 1 Million Women with Normal Cytological Findings. *The Journal of Infectious Diseases*, *202*(12), 1789–1799. https://doi.org/10.1086/657321

Buck, C. B., Day, P. M., & Trus, B. L. (2013). The Papillomavirus Major Capsid Protein L1. *Virology*, *445*(0), 169–174. https://doi.org/10.1016/j.virol.2013.05.038

Casalegno, J., Carval, K. L. B., Eibach, D., Valdeyron, M.-L., Lamblin, G., Jacquemoud, H.,

Mellier, G., Lina, B., Gaucherand, P., Mathevet, P., & Mekki, Y. (2012). High Risk HPV Contamination of Endocavity Vaginal Ultrasound Probes: An Underestimated Route of Nosocomial Infection? *PLOS ONE*, *7*(10), e48137. https://doi.org/10.1371/journal.pone.0048137

Castella, S., Bingham, G., & Sanders, C. M. (2006). Common determinants in DNA melting and helicase-catalysed DNA unwinding by papillomavirus replication protein E1. *Nucleic Acids Research*, *34*(10), 3008–3019. https://doi.org/10.1093/nar/gkl384

Castro-Muñoz, L. J., Manzo-Merino, J., Muñoz-Bello, J. O., Olmedo-Nieva, L., Cedro-Tanda, A., Alfaro-Ruiz, L. A., Hidalgo-Miranda, A., Madrid-Marina, V., & Lizano, M. (2019). The Human Papillomavirus (HPV) E1 protein regulates the expression of cellular genes involved in immune response. *Scientific Reports*, *9*(1), 13620. https://doi.org/10.1038/s41598-019-49886-4

Chelimo, C., Wouldes, T. A., Cameron, L. D., & Elwood, J. M. (2013). Risk factors for and prevention of human papillomaviruses (HPV), genital warts and cervical cancer. *Journal of Infection*, *66*(3), 207–217. https://doi.org/10.1016/j.jinf.2012.10.024

Cheng, L., Wang, Y., & Du, J. (2020). Human Papillomavirus Vaccines: An Updated Review. *Vaccines*, *8*(3), 391. https://doi.org/10.3390/vaccines8030391

Chesson, H. W., Dunne, E. F., Hariri, S., & Markowitz, L. E. (2014). The Estimated Lifetime Probability of Acquiring Human Papillomavirus in the United States. *Sexually Transmitted Diseases*, *41*(11), 660. https://doi.org/10.1097/OLQ.0000000000000193

Chojnacki, M., & Melendy, T. (2018). The HPV E2 Transcriptional Transactivation Protein Stimulates Cellular DNA Polymerase Epsilon. *Viruses*, *10*(6), 321. https://doi.org/10.3390/v10060321

Côté-Martin, A., Moody, C., Fradet-Turcotte, A., D'Abramo, C. M., Lehoux, M., Joubert, S., Poirier, G. G., Coulombe, B., Laimins, L. A., & Archambault, J. (2008). Human

Papillomavirus E1 Helicase Interacts with the WD Repeat Protein p80 To Promote Maintenance of the Viral Genome in Keratinocytes. *Journal of Virology*, *82*(3), 1271–1283. https://doi.org/10.1128/jvi.01405-07

Day, P. M., & Schelhaas, M. (2014). Concepts of papillomavirus entry into host cells. *Current Opinion in Virology*, *0*, 24–31. https://doi.org/10.1016/j.coviro.2013.11.002

De Geest, K., Turyk, M. E., Hosken, M. I., Hudson, J. B., Laimins, L. A., & Wilbanks, G. D. (1993). Growth and Differentiation of Human Papillomavirus Type 31b Positive Human Cervical Cell Lines. *Gynecologic Oncology*, *49*(3), 303–310. https://doi.org/10.1006/gyno.1993.1131

de Oliveira, C. M., Fregnani, J. H. T. G., & Villa, L. L. (2019). HPV Vaccine: Updates and Highlights. *Acta Cytologica*, *63*(2), 159–168. https://doi.org/10.1159/000497617

de Sanjosé, S., Brotons, M., & Pavón, M. A. (2018). The natural history of human papillomavirus infection. *Best Practice & Research Clinical Obstetrics & Gynaecology*, *47*, 2–13. https://doi.org/10.1016/j.bpobgyn.2017.08.015

de Sanjosé, S., Diaz, M., Castellsagué, X., Clifford, G., Bruni, L., Muñoz, N., & Bosch, F. X. (2007). Worldwide prevalence and genotype distribution of cervical human papillomavirus DNA in women with normal cytology: A meta-analysis. *The Lancet. Infectious Diseases*, *7*(7), 453–459. https://doi.org/10.1016/S1473-3099(07)70158-5

Del Pino, M., Vorsters, A., Joura, E. A., Doorbar, J., Haniszewski, M., Gudina, I. A., Kodjamanova, P., Velicer, C., & Drury, R. (2024). Risk factors for human papillomavirus infection and disease: A targeted literature summary. *Journal of Medical Virology*, *96*(2), e29420. https://doi.org/10.1002/jmv.29420

Della Fera, A. N., Warburton, A., Coursey, T. L., Khurana, S., & McBride, A. A. (2021). Persistent Human Papillomavirus Infection. *Viruses*, *13*(2), Article 2. https://doi.org/10.3390/v13020321

Dellal, H., Boulahtouf, A., Alaterre, E., Cuenant, A., Grimaldi, M., Bourguet, W., Gongora, C., Balaguer, P., & Pourquier, P. (2020). High Content Screening Using New U2OS Reporter Cell Models Identifies Harmol Hydrochloride as a Selective and Competitive Antagonist of the Androgen Receptor. *Cells*, *9*(6), 1469. https://doi.org/10.3390/cells9061469

Doorbar, J., Egawa, N., Griffin, H., Kranjec, C., & Murakami, I. (2015). Human papillomavirus molecular biology and disease association. *Reviews in Medical Virology*, *25*(Suppl Suppl 1), 2–23. https://doi.org/10.1002/rmv.1822

Doorbar, J., Quint, W., Banks, L., Bravo, I. G., Stoler, M., Broker, T. R., & Stanley, M. A. (2012). The Biology and Life-Cycle of Human Papillomaviruses. *Vaccine*, *30*, F55–F70. https://doi.org/10.1016/j.vaccine.2012.06.083

Dreer, M., van de Poel, S., & Stubenrauch, F. (2017). Control of viral replication and transcription by the papillomavirus E8^E2 protein. *Virus Research*, *231*, 96–102. https://doi.org/10.1016/j.virusres.2016.11.005

Ebrahimi, F., Rasizadeh, R., Jafari, S., & Baghi, H. B. (2024). Prevalence of HPV in anal cancer: Exploring the role of infection and inflammation. *Infectious Agents and Cancer*, *19*(1), 63. https://doi.org/10.1186/s13027-024-00624-0

Egawa, N., Egawa, K., Griffin, H., & Doorbar, J. (2015). Human Papillomaviruses; Epithelial Tropisms, and the Development of Neoplasia. *Viruses*, *7*(7), 3863–3890. https://doi.org/10.3390/v7072802

Egawa, N., Nakahara, T., Ohno, S.-I., Narisawa-Saito, M., Yugawa, T., Fujita, M., Yamato, K., Natori, Y., & Kiyono, T. (2012). The E1 protein of human papillomavirus type 16 is dispensable for maintenance replication of the viral genome. *Journal of Virology*, *86*(6), 3276–3283. https://doi.org/10.1128/JVI.06450-11

Evans, M. R., James, C. D., Loughran, O., Nulton, T. J., Wang, X., Bristol, M. L., Windle, B.,

& Morgan, I. M. (2017). A keratinocyte life cycle model identifies novel host genome regulation by human papillomavirus 16 relevant to HPV positive head and neck cancer. *Oncotarget*, *8*(47), 81892–81909. https://doi.org/10.18632/oncotarget.18328

Feng, Y., van Bodegraven, D., Kádek, A., L. B. Munguira, I., Soria-Martinez, L., Nentwich, S., Saha, S., Chardon, F., Kavan, D., Uetrecht, C., Schelhaas, M., & Roos, W. H. (2024). Glycan-induced structural activation softens the human papillomavirus capsid for entry through reduction of intercapsomere flexibility. *Nature Communications*, *15*(1), 10076. https://doi.org/10.1038/s41467-024-54373-0

Fujii, T., Brandsma, J. L., Peng, X., Srimatkandada, S., Li, L., Canaan, A., & Deisseroth, A. B. (2001). High and Low Levels of Cottontail Rabbit Papillomavirus E2 Protein Generate Opposite Effects on Gene Expression *. *Journal of Biological Chemistry*, *276*(2), 867–874. https://doi.org/10.1074/jbc.M007120200

Gallay, C., Miranda, E., Schaefer, S., Catarino, R., Jacot-Guillarmod, M., Menoud, P.-A., Guerry, F., Achtari, C., Sahli, R., Vassilakos, P., & Petignat, P. (2016). Human papillomavirus (HPV) contamination of gynaecological equipment. *Sexually Transmitted Infections*, *92*(1), 19–23. https://doi.org/10.1136/sextrans-2014-051977

Geimanen, J., Isok-Paas, H., Pipitch, R., Salk, K., Laos, T., Orav, M., Reinson, T., Ustav, M., Ustav, M., & Ustav, E. (2011). Development of a Cellular Assay System To Study the Genome Replication of High- and Low-Risk Mucosal and Cutaneous Human Papillomaviruses. *Journal of Virology*, *85*(7), 3315–3329. https://doi.org/10.1128/JVI.01985-10

Gheit, T. (2019). Mucosal and Cutaneous Human Papillomavirus Infections and Cancer Biology. *Frontiers in Oncology*, *9*, 355. https://doi.org/10.3389/fonc.2019.00355

Graham, S. V. (2016). Human Papillomavirus E2 Protein: Linking Replication, Transcription, and RNA Processing. *Journal of Virology*, *90*(19), 8384–8388.

https://doi.org/10.1128/jvi.00502-16

Graham, S. V. (2017a). Keratinocyte Differentiation-Dependent Human Papillomavirus Gene Regulation. *Viruses*, *9*(9), Article 9. https://doi.org/10.3390/v9090245

Graham, S. V. (2017b). The human papillomavirus replication cycle, and its links to cancer progression: A comprehensive review. *Clinical Science*, *131*(17), 2201–2221. https://doi.org/10.1042/CS20160786

Hasche, D., Stephan, S., Braspenning-Wesch, I., Mikulec, J., Niebler, M., Gröne, H.-J., Flechtenmacher, C., Akgül, B., Rösl, F., & Vinzón, S. E. (2017). The interplay of UV and cutaneous papillomavirus infection in skin cancer development. *PLOS Pathogens*, *13*(11), e1006723. https://doi.org/10.1371/journal.ppat.1006723

Hoffmann, R., Hirt, B., Bechtold, V., Beard, P., & Raj, K. (2006). Different Modes of Human Papillomavirus DNA Replication during Maintenance. *Journal of Virology*, *80*(9), 4431–4439. https://doi.org/10.1128/JVI.80.9.4431-4439.2006

Images Library DermNet. (n.d.). DermNet®. Retrieved April 25, 2025, from https://dermnetnz.org/images

Johansson, C., Somberg, M., Li, X., Backström Winquist, E., Fay, J., Ryan, F., Pim, D., Banks, L., & Schwartz, S. (2012). HPV-16 E2 contributes to induction of HPV-16 late gene expression by inhibiting early polyadenylation. *The EMBO Journal*, *31*(14), 3212–3227. https://doi.org/10.1038/emboj.2012.147

Karcher, S. (1991). Non-Radioactive DNA Hybridization Experiments for the Undergraduate Laboratory: The Southern Blot Analysis. *Test.Stud. Lab. Teach.*, *12*, 1–31.

Kasukawa, H., Howley, P. M., & Benson, J. D. (1998). A Fifteen-Amino-Acid Peptide Inhibits Human Papillomavirus E1-E2 Interaction and Human Papillomavirus DNA Replication In Vitro. *Journal of Virology*, *72*(10), 8166–8173. https://doi.org/10.1128/jvi.72.10.8166-8173.1998

Kuebler, U., Fischer, S., Mernone, L., Breymann, C., Abbruzzese, E., & Ehlert, U. (2021). Is stress related to the presence and persistence of oncogenic human papillomavirus infection in young women? *BMC Cancer*, *21*(1), 419. https://doi.org/10.1186/s12885-021-08010-4

Kurg, R. (2011). The Role of E2 Proteins in Papillomavirus DNA Replication. In *DNA Replication—Current Advances*. IntechOpen. https://doi.org/10.5772/19609

Lace, M. J., Anson, J. R., Thomas, G. S., Turek, L. P., & Haugen, T. H. (2008). The E8—E2 gene product of human papillomavirus type 16 represses early transcription and replication but is dispensable for viral plasmid persistence in keratinocytes. *Journal of Virology*, *82*(21), 10841–10853. https://doi.org/10.1128/JVI.01481-08

Lai, M.-C., Teh, B. H., & Tarn, W.-Y. (1999). A Human Papillomavirus E2 Transcriptional Activator: THE INTERACTIONS WITH CELLULAR SPLICING FACTORS AND POTENTIAL FUNCTION IN PRE-mRNA PROCESSING*. *Journal of Biological Chemistry*, *274*(17), 11832–11841. https://doi.org/10.1074/jbc.274.17.11832

Lambert, P. F., Münger, K., Rösl, F., Hasche, D., & Tommasino, M. (2020). Beta human papillomaviruses and skin cancer. *Nature*, *588*(7838), E20–E21. https://doi.org/10.1038/s41586-020-3023-0

Lee, B., Lee, S. W., Kim, D. I., & Kim, J. H. (2017). HPV prevalence in the foreskins of asymptomatic healthy infants and children: Systematic review and meta-analysis. *Scientific Reports*, *7*, 7050. https://doi.org/10.1038/s41598-017-07506-z

Lee, D., Sohn, H., Kalpana, G. V., & Choe, J. (1999). Interaction of E1 and hSNF5 proteins stimulates replication of human papillomavirus DNA. *Nature*, *399*(6735), 487–491. https://doi.org/10.1038/20966

Lee, M., Gerend, M. A., Whittington, K. D., Collins, S. K., McKinney, S. L., Franca, M. C., Boyer, V. E., McKinnies, R. C., Chen, C.-C., Villegas, J., & Adjei Boakye, E. (2024).

Factors associated with HPV-associated sexual risk behaviors among sexually active college students. *Journal of Behavioral Medicine*, *47*(2), 334–341. https://doi.org/10.1007/s10865-023-00463-1

Lototskaja, E., Liblekas, L., Piirsoo, M., Laaneväli, A., Ibragimov, R., & Piirsoo, A. (2023). Phosphorylation of E2 Serine Residue 402 Is Required for the Transcription and Replication of the HPV5 Genome. *Journal of Virology*, *97*(6), e0064323. https://doi.org/10.1128/jvi.00643-23

Lototskaja, E., Sahharov, O., Piirsoo, M., Kala, M., Ustav, M., & Piirsoo, A. (2021). Cyclic AMP-Dependent Protein Kinase Exhibits Antagonistic Effects on the Replication Efficiency of Different Human Papillomavirus Types. *Journal of Virology*, *95*(13), e0025121. https://doi.org/10.1128/JVI.00251-21

Mammas, I. N., Dalianis, T., Doukas, S. G., Zaravinos, A., Achtsidis, V., Thiagarajan, P., Theodoridou, M., & Spandidos, D. A. (2019). Paediatric virology and human papillomaviruses: An update. *Experimental and Therapeutic Medicine*, *17*(6), 4337–4343. https://doi.org/10.3892/etm.2019.7516

McBride, A. A. (2013). The Papillomavirus E2 Proteins. *Virology*, *445*(0), 57–79. https://doi.org/10.1016/j.virol.2013.06.006

McBride, A. A. (2017). Mechanisms and strategies of papillomavirus replication. *Biological Chemistry*, *398*(8), 919–927. https://doi.org/10.1515/hsz-2017-0113

McBride, A. A. (2022). Human papillomaviruses: Diversity, infection and host interactions. *Nature Reviews Microbiology*, *20*(2), 95–108. https://doi.org/10.1038/s41579-021-00617-5

McBride, A. A. (2024a). Human malignancies associated with persistent HPV infection. *The Oncologist*, *29*(6), 457–464. https://doi.org/10.1093/oncolo/oyae071

McBride, A. A. (2024b). Human malignancies associated with persistent HPV infection. *The*

Oncologist, *29*(6), 457–464. https://doi.org/10.1093/oncolo/oyae071

McBride, A. A., Byrne, J. C., & Howley, P. M. (1989). E2 polypeptides encoded by bovine papillomavirus type 1 form dimers through the common carboxyl-terminal domain: Transactivation is mediated by the conserved amino-terminal domain. *Proceedings of the National Academy of Sciences*, *86*(2), 510–514. https://doi.org/10.1073/pnas.86.2.510

McBride, A. A., Schlegel, R., & Howley, P. M. (1988). The carboxy‐terminal domain shared by the bovine papillomavirus E2 transactivator and repressor proteins contains a specific DNA binding activity. *The EMBO Journal*, *7*(2), 533–539. https://doi.org/10.1002/j.1460-2075.1988.tb02842.x

Mlynarczyk-Bonikowska, B., & Rudnicka, L. (2024). HPV Infections—Classification, Pathogenesis, and Potential New Therapies. *International Journal of Molecular Sciences*, *25*(14), 7616. https://doi.org/10.3390/ijms25147616

Mohr, I. J., Clark, R., Sun, S., Androphy, E. J., MacPherson, P., & Botchan, M. R. (1990). Targeting the E1 Replication Protein to the Papillomavirus Origin of Replication by Complex Formation with the E2 Transactivator. *Science*, *250*(4988), 1694–1699. https://doi.org/10.1126/science.2176744

Morin, G., Fradet-Turcotte, A., Di Lello, P., Bergeron-Labrecque, F., Omichinski, J. G., & Archambault, J. (2011). A Conserved Amphipathic Helix in the N-Terminal Regulatory Region of the Papillomavirus E1 Helicase Is Required for Efficient Viral DNA Replication. *Journal of Virology*, *85*(11), 5287–5300. https://doi.org/10.1128/JVI.01829-10

Munday, J. S., Thomson, N. A., & Luff, J. A. (2017). Papillomaviruses in dogs and cats. *The Veterinary Journal*, *225*, 23–31. https://doi.org/10.1016/j.tvjl.2017.04.018

Munoz, I. M., Szyniarowski, P., Toth, R., Rouse, J., & Lachaud, C. (2014). Improved

Genome Editing in Human Cell Lines Using the CRISPR Method. *PLOS ONE*, *9*(10), e109752. https://doi.org/10.1371/journal.pone.0109752

Murakami, I., Egawa, N., Griffin, H., Yin, W., Kranjec, C., Nakahara, T., Kiyono, T., & Doorbar, J. (2019). Roles for E1-independent replication and E6-mediated p53 degradation during low-risk and high-risk human papillomavirus genome maintenance. *PLoS Pathogens*, *15*(5), e1007755. https://doi.org/10.1371/journal.ppat.1007755

Myers, D. J., Kwan, E., & Fillman, E. P. (2025). Epidermodysplasia Verruciformis. In *StatPearls*. StatPearls Publishing. http://www.ncbi.nlm.nih.gov/books/NBK534198/

Nahidi, M., Nahidi, Y., Saghebi, A., Kardan, G., Jarahi, L., Aminzadeh, B., Shojaei, P., & Bordbar, M. R. F. (2018). Evaluation of Psychopathology and Quality of Life in Patients with Anogenital Wart Compared to Control Group. *Iranian Journal of Medical Sciences*, *43*(1), 65–69.

Oliveira, J. G., Colf, L. A., & McBride, A. A. (2006). Variations in the association of papillomavirus E2 proteins with mitotic chromosomes. *Proceedings of the National Academy of Sciences*, *103*(4), 1047–1052. https://doi.org/10.1073/pnas.0507624103

Parish, J. L., Kowalczyk, A., Chen, H.-T., Roeder, G. E., Sessions, R., Buckle, M., & Gaston, K. (2006). E2 Proteins from High- and Low-Risk Human Papillomavirus Types Differ in Their Ability To Bind p53 and Induce Apoptotic Cell Death. *Journal of Virology*, *80*(9), 4580–4590. https://doi.org/10.1128/JVI.80.9.4580-4590.2006

Patel, T., Morrison, L. K., Rady, P., & Tyring, S. (2010). Epidermodysplasia Verruciformis and Susceptibility to HPV. *Disease Markers*, *29*(3–4), 199–206. https://doi.org/10.1155/2010/345436

PaVE. (n.d.). Retrieved May 7, 2025, from https://pave.niaid.nih.gov/explore/reference_genomes

Petca, A., Borislavschi, A., Zvanca, M. E., Petca, R.-C., Sandru, F., & Dumitrascu, M. C. (2020). Non-sexual HPV transmission and role of vaccination for a better future (Review). *Experimental and Therapeutic Medicine*, *20*(6), 1–1. https://doi.org/10.3892/etm.2020.9316

Pett, M. R., Alazawi, W. O. F., Roberts, I., Dowen, S., Smith, D. I., Stanley, M. A., & Coleman, N. (2004). Acquisition of high-level chromosomal instability is associated with integration of human papillomavirus type 16 in cervical keratinocytes. *Cancer Research*, *64*(4), 1359–1368. https://doi.org/10.1158/0008-5472.can-03-3214

Piirsoo, A., Kala, M., Sankovski, E., Ustav, M., & Piirsoo, M. (2020). Uncovering the Role of the E1 Protein in Different Stages of Human Papillomavirus 18 Genome Replication. *Journal of Virology*, *94*(20), e00674-20. https://doi.org/10.1128/JVI.00674-20

Piirsoo, A., Piirsoo, M., Kala, M., Sankovski, E., Lototskaja, E., Levin, V., Salvi, M., & Ustav, M. (2019). Activity of CK2α protein kinase is required for efficient replication of some HPV types. *PLOS Pathogens*, *15*(5), e1007788. https://doi.org/10.1371/journal.ppat.1007788

Qi, S.-Z., Wang, S.-M., Shi, J.-F., Wang, Q.-Q., Chen, X.-S., Sun, L.-J., Liu, A., Zhang, N., Jiang, N., Siva, P., Xu, X.-L., & Qiao, Y.-L. (2014). Human papillomavirus-related psychosocial impact of patients with genital warts in China: A hospital-based cross-sectional study. *BMC Public Health*, *14*(1), 739. https://doi.org/10.1186/1471-2458-14-739

Ramoz, N., Rueda, L.-A., Bouadjar, B., Montoya, L.-S., Orth, G., & Favre, M. (2002). Mutations in two adjacent novel genes are associated with epidermodysplasia verruciformis. *Nature Genetics*, *32*(4), 579–581. https://doi.org/10.1038/ng1044

Razzaghi, H., Saraiya, M., Thompson, T. D., Henley, S. J., Viens, L., & Wilson, R. (2018). Five-year relative survival for human papillomavirus-associated cancer sites. *Cancer*,

124(1), 203–211. https://doi.org/10.1002/cncr.30947

Rector, A., & Van Ranst, M. (2013). Animal papillomaviruses. *Virology*, *445*(1), 213–223. https://doi.org/10.1016/j.virol.2013.05.007

Rehm, T. M., Straub, E., Iftner, T., & Stubenrauch, F. (2022). Restriction of viral gene expression and replication prevents immortalization of human keratinocytes by a beta-human papillomavirus. *Proceedings of the National Academy of Sciences*, *119*(11), e2118930119. https://doi.org/10.1073/pnas.2118930119

Rollison, D. E., Viarisio, D., Amorrortu, R. P., Gheit, T., & Tommasino, M. (2019). An Emerging Issue in Oncogenic Virology: The Role of Beta Human Papillomavirus Types in the Development of Cutaneous Squamous Cell Carcinoma. *Journal of Virology*. https://doi.org/10.1128/jvi.01003-18

Roman, A., & Munger, K. (2013). The papillomavirus E7 proteins. *Virology*, *445*(0), 138–168. https://doi.org/10.1016/j.virol.2013.04.013

Sanders, C. M., & Stenlund, A. (1998). Recruitment and loading of the E1 initiator protein: An ATP-dependent process catalysed by a transcription factor. *The EMBO Journal*, *17*(23), 7044–7055. https://doi.org/10.1093/emboj/17.23.7044

Sanders, C. M., & Stenlund, A. (2000). Transcription Factor-dependent Loading of the E1 Initiator Reveals Modular Assembly of the Papillomavirus Origin Melting Complex *. *Journal of Biological Chemistry*, *275*(5), 3522–3534. https://doi.org/10.1074/jbc.275.5.3522

Sankovski, E., Männik, A., Geimanen, J., Ustav, E., & Ustav, M. (2014). Mapping of Betapapillomavirus Human Papillomavirus 5 Transcription and Characterization of Viral-Genome Replication Function. *Journal of Virology*, *88*(2), 961–973. https://doi.org/10.1128/JVI.01841-13

Sprague, D. L., Phillips, S. L., Mitchell, C. J., Berger, K. L., Lace, M., Turek, L. P., &

Klingelhutz, A. J. (2002). Telomerase Activation in Cervical Keratinocytes Containing Stably Replicating Human Papillomavirus Type 16 Episomes. *Virology*, *301*(2), 247–254. https://doi.org/10.1006/viro.2002.1542

Stanley, M. A., Browne, H. M., Appleby, M., & Minson, A. C. (1989). Properties of a non-tumorigenic human cervical keratinocyte cell line. *International Journal of Cancer*, *43*(4), 672–676. https://doi.org/10.1002/ijc.2910430422

Steger, G., & Corbach, S. (1997). Dose-dependent regulation of the early promoter of human papillomavirus type 18 by the viral E2 protein. *Journal of Virology*, *71*(1), 50–58. https://doi.org/10.1128/jvi.71.1.50-58.1997

Sun-Kuie, T., Tew-Hongw, H., & Soo-Kim, L.-T. (1990). Is Genital Human Papillomavirus Infection Always Sexually Transmitted? *Australian and New Zealand Journal of Obstetrics and Gynaecology*, *30*(3), 240–242. https://doi.org/10.1111/j.1479-828X.1990.tb03223.x

Swindle, C. S., & Engler, J. A. (1998). Association of the human papillomavirus type 11 E1 protein with histone H1. *Journal of Virology*, *72*(3), 1994–2001. https://doi.org/10.1128/JVI.72.3.1994-2001.1998

Uberoi, A., Yoshida, S., Frazer, I. H., Pitot, H. C., & Lambert, P. F. (2016). Role of Ultraviolet Radiation in Papillomavirus-Induced Disease. *PLOS Pathogens*, *12*(5), e1005664. https://doi.org/10.1371/journal.ppat.1005664

Van Doorslaer, K., & McBride, A. A. (2016). Molecular archeological evidence in support of the repeated loss of a papillomavirus gene. *Scientific Reports*, *6*(1), 33028. https://doi.org/10.1038/srep33028

Vande Pol, S. B., & Klingelhutz, A. J. (2013). Papillomavirus E6 oncoproteins. *Virology*, *445*(0), 115–137. https://doi.org/10.1016/j.virol.2013.04.026

Wang, J. W., & Roden, R. B. S. (2013). L2, the minor capsid protein of papillomavirus.

Virology, *445*(0), 175–186. https://doi.org/10.1016/j.virol.2013.04.017

White, P. W., Titolo, S., Brault, K., Thauvette, L., Pelletier, A., Welchner, E., Bourgon, L., Doyon, L., Ogilvie, W. W., Yoakim, C., Cordingley, M. G., & Archambault, J. (2003). Inhibition of Human Papillomavirus DNA Replication by Small Molecule Antagonists of the E1-E2 Protein Interaction*. *Journal of Biological Chemistry*, *278*(29), 26765–26772. https://doi.org/10.1074/jbc.M303608200

Zhao, K.-N., Hengst, K., Liu, W.-J., Liu, Y. H., Liu, X. S., McMillan, N. A. J., & Frazer, I. H. (2000). BPV1 E2 Protein Enhances Packaging of Full-Length Plasmid DNA in BPV1 Pseudovirions. *Virology*, *272*(2), 382–393. https://doi.org/10.1006/viro.2000.0348

Zou, N., Lin, B. Y., Duan, F., Lee, K.-Y., Jin, G., Guan, R., Yao, G., Lefkowitz, E. J., Broker, T. R., & Chow, L. T. (2000). The Hinge of the Human Papillomavirus Type 11 E2 Protein Contains Major Determinants for Nuclear Localization and Nuclear Matrix Association. *Journal of Virology*, *74*(8), 3761–3770. https://doi.org/10.1128/jvi.74.8.3761-3770.2000

NON-EXCLUSIVE LICENCE TO REPRODUCE THE THESIS AND MAKE THE THESIS PUBLIC

I, Sofiya Babok,

1. grant the University of Tartu a free permit (non-exclusive licence) to

   reproduce, for the purpose of preservation, including for adding to the digital archives of the University of Tartu until the expiry of the term of copyright, my thesis

   "The role of the viral E1 and E2 proteins in the stable replication of human papillomavirus type 5 genome", supervised by Assoc. Prof. Dr. Alla Piirsoo;

2. grant the University of Tartu the permit to make the thesis specified in point 1 available to the public via the web environment of the University of Tartu, including via the digital archives, under the Creative Commons licence CC BY NC ND 4.0, which allows, by giving appropriate credit to the author, to reproduce, distribute the work and communicate it to the public, and prohibits the creation of derivative works and any commercial use of the work from ***20/05/2025*** until the expiry of the term of copyright;
3. am aware that the author retains the rights specified in points 1 and 2;
4. confirm that granting the non-exclusive licence does not infringe other persons' intellectual property rights or rights arising from the personal data protection legislation.

Sofiya Babok

20/05/2025